Nonlinear Infrared Spectroscopy

H. J. Bakker

FOM Institute for Atomic and Molecular Physics, Science Park 104, 1098 XG Amsterdam, The

Netherlands

(December 18, 2009)

I. VIBRATIONAL SPECTROSCOPY

The part of the electromagnetic spectrum that is resonant with molecular vibrations is the infrared. It includes wavelengths ranging from 1 μm to 100 μm. At longer wavelengths (100 μm to 1 cm) lies the domain of rotational spectroscopy, which uses the microwave part of the spectrum to study rotational transitions in molecules. At shorter wavelengths (10 nm to 1 μm) the visible and ultraviolet regions of the spectrum can be found, which induce electronic transitions in molecules; hence comes the name electronic spectroscopy. Figure 1 illustrates the physical processes underlying these types of spectroscopy using the diatomic molecule as an example.
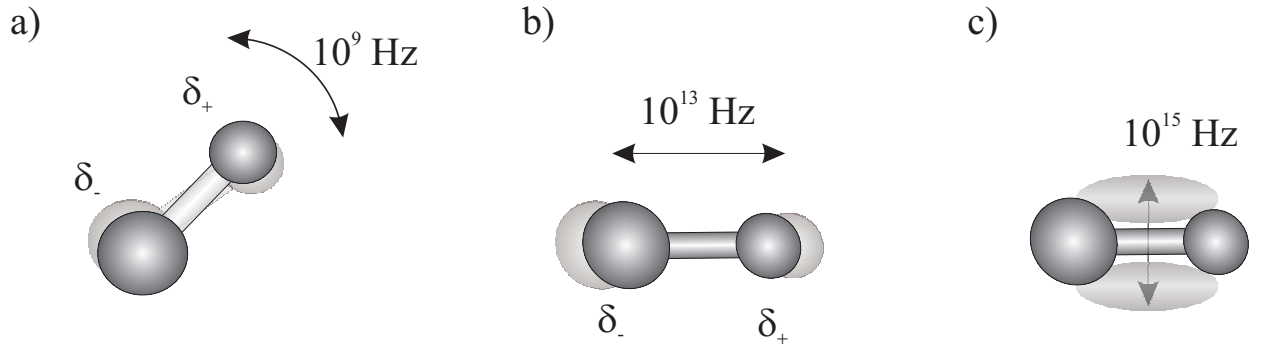
FIG. 1. The three degrees of freedom of a diatomic molecule that form the basis for rotational, vibrational and electronic spectroscopy. For molecules that are composed of two different atoms the binding electrons will not be divided equally among the two atoms, which leads to partial charges on the two atoms (δ_+ and δ_-). a) The rotational motion of the molecule causes these two charges to oscillate, thus providing a coupling with microwave radiation. b) The vibrational motion of the nuclei occurs at higher frequencies and leads to a charge oscillation that is resonant with infrared radiation. c) The interaction of optical radiation with the electrons constituting the chemical bond between the two atoms forms the basis for electronic spectroscopy.

II. VIBRATIONAL SPECTROSCOPY OF HYDROGEN-BONDED SYSTEMS

Hydrogen bonds arise when hydrogen is covalently bound to an electronegative element, such as O, N or F. The binding electrons are drawn towards the electronegative atom, and this causes the hydrogen atom to acquire a small positive charge. As a result, the hydrogen atom is attracted to the lone pairs of other electronegative elements. The hydrogen bond is a motif that is encountered everywhere in living nature, not only in liquid water. The majority of biological macromolecules, such as DNA and proteins, are shaped by hydrogen bonds (figure 2), which, in addition to structuring these macromolecules, also provide them with the flexibility they need to function properly.
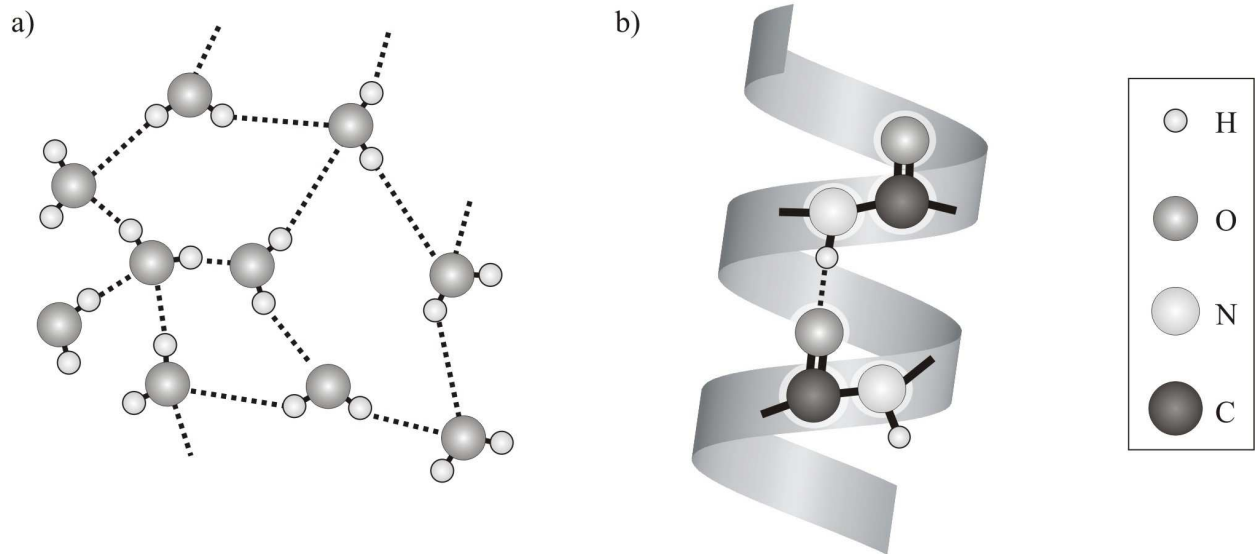
FIG. 2. a) Tetrahedral structure of liquid water. The hydrogen bonds are represented as dotted lines. b) The alpha-helix, a structural motif in proteins, is held together by hydrogen bonds between the amide groups of different amino acids.

In liquid water hydrogen bonds of the type $OH\cdots O$ are responsible for the strong attraction between water molecules. A water molecule can engage into a maximum of four hydrogen bonds; it can accept two hydrogen bonds and simultaneously donate two. In ice this maximum number of hydrogen bonds is indeed formed, which leads to a tetrahedral structure in which every water molecule is fourfold coordinated by other water molecules. In the liquid phase the ordered structure collapses and acquires some degree of disorder. Locally, however, the average tetrahedral coordination is retained (figure 2a) and liquid water is said to be a highly coordinated and structured liquid. Other hydrogen bonded liquids than water exist, such as methanol, but water is unique in its ability to form a three-dimensional network of hydrogen bonds. This three-dimensional hydrogen-bond network is highly dynamic: hydrogen bonds stretch, contract, break and reform on a picosecond timescale.

Infrared spectroscopy can be used for studying water and other hydrogen-bonded systems. Figure 3 shows the mid-infrared spectrum of water. This region of the spectrum is

sensitive to molecular vibrations. In the spectrum two resonances can be discerned: one around 1600 cm^{-1}, which is due to the HOH bending vibration, and one around 3400 cm^{-1} due to the two OH stretching vibrations. The OH stretching vibration is particularly well suited to study hydrogen bonding, as its frequency provides direct information about the hydrogen-bond strength: the stronger the hydrogen bonds, the lower the OH stretching frequency. In liquid water many different conformations of water molecules exist, some of which are strongly hydrogen bonded, others which are weakly hydrogen bonded. These conformations absorb at different frequencies, which causes the large spectral width of the OH-stretching absorption. The band is said to be inhomogeneously broadened.[1] Because of the rapid interconversion of different hydrogen-bonded conformations, conventional (linear) infrared spectroscopy can only obtain time-averaged information about the structure of water. In order to obtain dynamic information one has to resort to nonlinear spectroscopic techniques, which use ultrashort laser pulses ($\sim$100 fs) to obtain instantaneous snapshots of the hydrogen bond structure. In this thesis we will use one of these techniques, mid-infrared pump-probe spectroscopy, to study the dynamical aspects of hydrogen bonding in pure water and other systems. An advantage of mid-infrared pump-probe spectroscopy is that, when it is performed in a polarization-resolved manner, it also allows one to monitor the rotational *motion* of water molecules, and we will make extensive use of this property. In fact, the central question in this thesis is how the motion of water molecules is affected by hydrogen bonds and by the nearby presence of other molecules.

———

[1]An additional factor contributing to the width of the OH-stretching band is the coupling of the two OH vibrations of H_2O, which leads to a symmetric and antisymmetric combination which absorb at different frequencies.
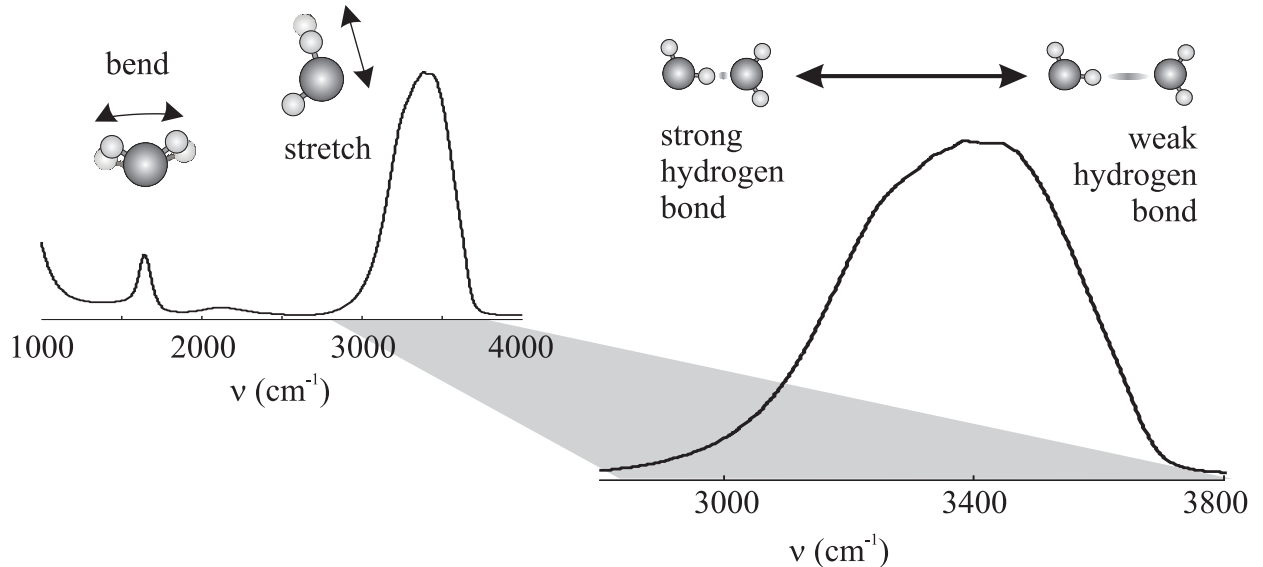
FIG. 3. Mid-infrared spectrum of water which shows the absorption due to the bending and stretching vibrations of the water molecule. The OH-stretching vibration is strongly inhomogeneously broadened as a result of the hydrogen-bond interaction. There is a strong correlation between the hydrogen-bond strength of a water molecule and its OH-stretching frequency. Strongly bound water molecules absorb on the low-frequency side of the spectrum, and weakly bound water molecules absorb on the high-frequency side.

III. THE HARMONIC OSCILLATOR

The vibrations of molecules can be described as a collection of quantum mechanical harmonic oscillators. Figure 4a displays the simplest possible example of a harmonic oscillator: a particle of mass m that is connected to a body of infinite mass by spring with spring constant k. This system has the following Hamiltonian

$$\hat{H}_0 = \frac{\hat{p}^2}{2m} + \frac{1}{2}k\hat{x}^2, \tag{1}$$

where $\hat{p}$ and $\hat{x}$ are the momentum and position operators.[2] Of course, this is an idealized system that is very different from a real molecule; however, it is convenient because more

———

[2]Quantum mechanical operators will be denoted by a hat $\hat{}$.

6

complex systems, such as diatomic and polyatomic molecules, are described by Hamiltonians of the same form. Clearly for these systems the parameters in eqn. 1 have to be interpreted in a different way. For a diatomic molecule the mass m no longer represents the particle mass but rather the reduced mass of the two atoms (figure 4b). In the case of polyatomic molecules the situation is more complex because we have to take into account the fact that multiple atoms move at the same time. By working with normal mode coordinates, however, a vibration can still be described by a single displacement coordinate x . A normal mode coordinate describes the synchronous displacement of all atoms during the course of a vibration. As an example figure 4c shows the antisymmetric vibration of H_2O. For polyatomic molecules the mass m in eqn. 1 represents the effective mass of the vibration, which is a measure for the amount of mass that moves around during the vibration and is generally a complicated expression of the atomic masses.
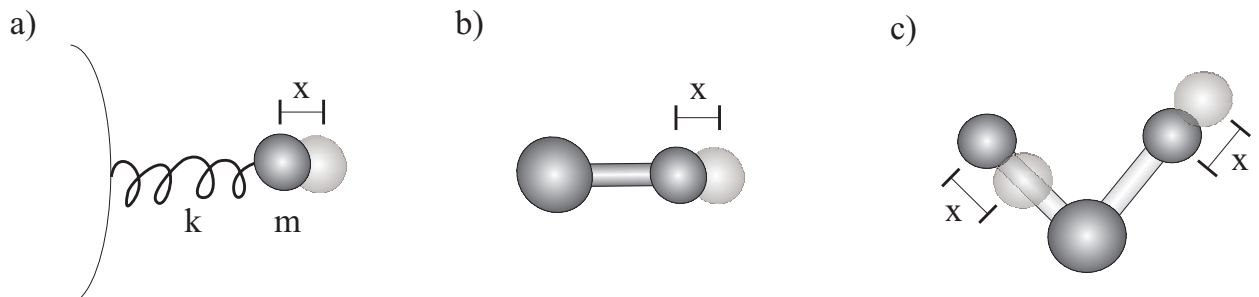

FIG. 4. a) The harmonic oscillator. A particle of mass m is attached to a body of infinite mass by an ideal spring with spring constant k. The vibrations of molecules can be described by harmonic oscillators provided that certain substitutions are made. b) For the diatomic molecule the only change is that the mass m of the oscillator should be replaced by the reduced mass of the system $(m_1 m_2/(m_1 + m_2))$. c) Vibrations of polyatomic molecules are described in terms of normal modes. Here the antisymmetric mode of H_2O is shown. Such a vibration can still be described by a single coordinate, which represents a linear combination of the atomic displacements during the vibration.

We now consider the solutions to the harmonic oscillator. The allowed states $|\phi\rangle$ follow from the time-independent Schrödinger equation:

7

$$\hat{H}|\phi\rangle = E|\phi\rangle, \tag{2}$$

where E is the total energy. In more detail:

$$-\left(\frac{\hbar^2}{2m}\right)\left(\frac{d^2\phi(x)}{dx^2}\right) + \frac{1}{2}kx^2\phi(x) = E\phi(x), \tag{3}$$

with $\hbar = h/2\pi$, $\phi(x)$ the wave function, $k = m\omega^2$ the spring constant, ω the angular frequency $(=2\pi\nu)$. The solutions are $\phi_v(x) = N_v H_v(y)e^{-y^2/2}$ with $y = \sqrt{m\omega/\hbar}x$, N_v a normalisation constant H_v a Hermite polynomial. The eigenenergies are given by

$$E_v = \hbar\omega_0(v + \frac{1}{2}), \tag{4}$$

where $\omega_0 = \sqrt{k/m}$ represents the resonance frequency of the classical oscillator and v the vibrational quantum number. A wavefunction $|\phi_v\rangle$, which we will also denote as $|v\rangle$, is associated with every eigenenergy E_v. We see that the energies are equally spaced, as shown in figure 5.
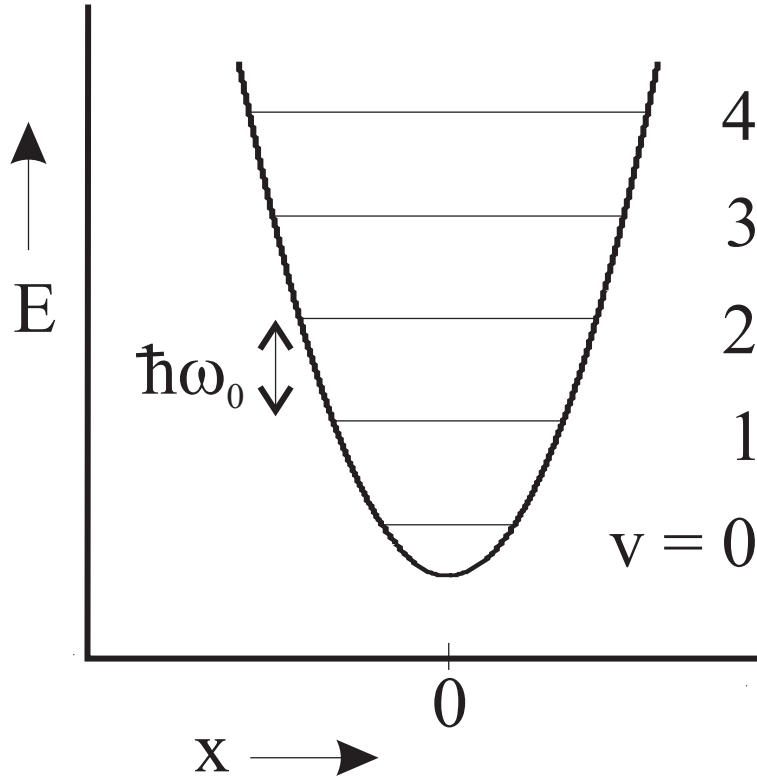

FIG. 5. Energy level diagram of the harmonic oscillator.

For the transition dipole matrix elements we have

$$\langle \phi_v | x | \phi_v \rangle = 0 \tag{5}$$

and:

$$\langle \phi_v | x | \phi_{v-1} \rangle \sim \sqrt{v} \tag{6}$$

A. What is oscillating with a quantum harmonic oscillator?

Is $\langle x \rangle$ time dependent? To answer this question one has to evaluate $\langle x \rangle = \int_{-\infty}^{\infty} dx \psi^*(x,t) x \psi(x,t)$. This can be done with the time-dependent Schrödinger equation:

$$H\psi = i\hbar \frac{d\psi}{dt} \tag{7}$$

When the Hamilton operator $\left(=-\left(\frac{\hbar^2}{2m}\right)\left(\frac{d^2}{dx^2}\right) + \frac{1}{2}kx^2\right)$ is not time dependent:

$$\psi(x,t) = C_v \phi_v e^{-E_v t/\hbar} \tag{8}$$

Expectation value $\langle x \rangle$ for $\psi(x,t) = \phi_0(x) e^{-iE_0 t/\hbar}$ (ground state):

$$\int_{-\infty}^{\infty} dx \phi_0^*(x) e^{iE_0 t/\hbar} x \phi_0(x) e^{-iE_0 t/\hbar} = \langle \phi_0 | x | \phi_0 \rangle = 0. \tag{9}$$

Expectation value for $\psi(x,t) = \phi_1(x) e^{-iE_1 t/\hbar}$:

$$\int_{-\infty}^{\infty} dx \phi_1^*(x) e^{iE_1 t/\hbar} x \phi_1(x) e^{-iE_1 t/\hbar} = \langle \phi_1 | x | \phi_1 \rangle = 0. \tag{10}$$

Expectation value for $\psi(x,t) = C_0 \phi_0(x) e^{-iE_0 t/\hbar} + C_1 \phi_1(x) e^{-iE_1 t/\hbar}$:

$$\langle \psi(x,t) | x | \psi(x,t) \rangle = C_0^* C_0 \langle \phi_0 | x | \phi_0 \rangle + C_1^* C_1 \langle \phi_1 | x | \phi_1 \rangle + \tag{11}$$

$$C_0^* C_1 \langle \phi_0 | x | \phi_1 \rangle e^{-i(E_1 - E_0)t/\hbar} + C_1^* C_0 \langle \phi_1 | x | \phi_0 \rangle e^{i(E_1 - E_0)t/\hbar} =$$

$$2\left[C_0^* C_1 \langle \phi_0 | x | \phi_1 \rangle + c.c \right] \cos(\omega t)$$

B. Transitions for a quantum harmonic oscillator

Transitions between the energy levels can be induced by applying a time-dependent perturbation to the Hamiltonian. In the case of a vibrating molecule, irradiation with infrared light provides such perturbation. The effect of such a perturbation can be described with the time-dependent Schrödinger equation,

$$i\hbar\frac{\partial}{\partial t}|\phi\rangle = \hat{H}|\phi\rangle. \tag{12}$$

The Hamiltonian is the sum of the unperturbed Hamiltonian $\hat{H}_0$ and the time-dependent perturbation $\hat{V}_{\text{int}}(t)$,

$$\hat{H} = \hat{H}_0 + \hat{V}_{\text{int}}(t). \tag{13}$$

We will assume that the perturbation varies harmonically with time,

$$\hat{V}_{\text{int}} = \hat{V}(e^{i\omega t} + e^{-i\omega t}), \tag{14}$$

as this is the form of the light-matter interaction if the coupling $\hat{V}$ is written as

$$\hat{V} = -\frac{1}{2}\vec{\hat{\mu}} \cdot \vec{E}_0. \tag{15}$$

Here $\vec{\hat{\mu}}$ is the dipole moment operator. In the above equation we have used the electric-dipole approximation and assumed the following expression for the oscillating electric field

$$\vec{E}(t) = \vec{E}_0 \cos \omega t, \tag{16}$$

$$= \frac{1}{2}\vec{E}_0(e^{i\omega t} + e^{-i\omega t}). \tag{17}$$

Fermi's golden rule gives the rate W_{kl} at which transitions occur from state $|l\rangle$ to $|k\rangle$

$$W_{kl} = \frac{2\pi}{\hbar^2}|\langle k|\hat{V}|l\rangle|^2 \left[\delta(\omega_{kl} - \omega) + \delta(\omega_{kl} + \omega)\right], \tag{18}$$

where $\omega_{kl} = (E_k - E_l)/\hbar$. The delta functions ensure that transitions occur only when the photon energy $\hbar\omega$ matches the energy difference between the states. A result of Fermi's

golden rule is that the probability of light absorption equals the probability of stimulated emission.

If we explicitly write out the coupling term in the above equation, we obtain

$$W_{kl} = \frac{\pi}{2\hbar^2} |\langle k | \vec{E}_0 \cdot \vec{\hat{\mu}} | l \rangle|^2, \tag{19}$$

$$= \frac{\pi E_0^2}{2\hbar^2} \cos^2(\theta) \mu_{kl}^2, \tag{20}$$

where we have assumed resonant excitation. The quantity $\vec{\mu}_{kl} = |\langle k | \vec{\hat{\mu}} | l \rangle|$ is called the transition dipole moment; it is the molecular quantity that determines the strength of an absorption. θ is the angle between the transition dipole moment and the electric field polarization. We see that transitions are most likely to occur if the radiation is polarized parallel to the transition dipole moment.

As it stands the above equation can refer to any type of dipolar transition. In order to have it refer to a vibrational transition we need to specify the form of the dipole moment operator. This operator depends on the electronic wave function but we can obtain a useful phenomenological expression by expanding it as a function of the vibrational coordinate x

$$\vec{\hat{\mu}} \approx \vec{\mu}_0 + \hat{x} \frac{\partial \vec{\mu}}{\partial x}. \tag{21}$$

Note that the operator character has been switched from $\vec{\hat{\mu}}$ to $\hat{x}$. If we use this expression for the dipole moment, we arrive at

$$W_{kl} = \frac{\pi E_0^2}{2\hbar^2} \cos^2 \theta \left(\frac{\partial \vec{\mu}}{\partial x} \right)^2 |\langle k | \hat{x} | l \rangle|^2. \tag{22}$$

This expression contains a number of factors, each of which represents a selection rule in vibrational spectroscopy. Below we summarize these selection rules:

- $W_{kl} \propto \left(\frac{\partial \vec{\mu}}{\partial x} \right)^2$

  A vibration is only infrared active if the vibrational motion leads to a change in the dipole moment. As a consequence symmetric vibrations, such as the vibrations of O_2 and N_2 and the symmetric stretching vibration of CH_4 are not observed in infrared spectroscopy.

11

- $W_{kl} \propto |\langle k|\hat{x}|l\rangle|^2$

  In the harmonic approximation the matrix element $\langle k|\hat{x}|l\rangle$ is only non-zero for $l = k\pm 1$. As a consequence the only allowed transitions are those that change the excitation of the oscillator by one quantum of energy. There are two effects that can lead to a relaxation of this selection rule. The first is an anharmonicity in the potential energy of the oscillator (i.e. the presence of higher order terms in the potential energy: $\sim x^3$, $\sim x^4$, etc.). This mechanical anharmonicity leads to the coupling of wave functions for which $|l - k| > 1$. A second possibility is the presence of quadratic and higher order terms in the expansion of the dipole moment (eqn. 21). Higher order coupling terms of the form $\hat{x}^n$ lead to the coupling of states for which $|l - k| = n$. This kind of anharmonicity is known as electrical anharmonicity. In general multiple-quantum transitions are much weaker than single-quantum transitions.

- $W_{kl} \propto \cos^2(\theta)$

  Only the electric field component parallel to the transition dipole moment (i.e. in the direction of change of the dipole moment) can induce transitions. No transitions can occur if the radiation is polarized perpendicular to the transition dipole.

IV. LAMBERT-BEER'S LAW

Fermi's golden rule provides a microscopic expression for the rate at which energy is absorbed from a beam of light. In this section we relate this equation to a macroscopic expression for the attenuation of the light beam. We begin with the expression for the intensity I in terms of the amplitude of the electric field (eqn. 16)

$$I(\omega) = \frac{1}{2}c\epsilon_0 E_0^2(\omega). \tag{23}$$

Here c is the speed of light and ϵ_0 is the permittivity of free space. In terms of the intensity we can write the transition rate from eqn. 20 as

$$W_{kl} = \frac{\pi I(\omega_{kl})}{3\hbar^2 c \epsilon_0} \mu_{kl}^2, \tag{24}$$

where we have assumed that the sample is isotropic so that we can replace $\cos^2 \theta$ by its average value of $\frac{1}{3}$. The rate at which energy is absorbed from a beam of light by a single molecule is found by multiplying the transition rate by the photon energy

$$P(\omega_{kl}) = \hbar \omega_{kl} W_{kl}. \tag{25}$$

In writing this equation we have assumed that the population of the excited state is negligible compared to the ground state population. Since the absorbed power is proportional to the intensity of the light beam, we can define a new molecular quantity, the absorption cross section σ, as the absorbed power scaled to the intensity of the light,

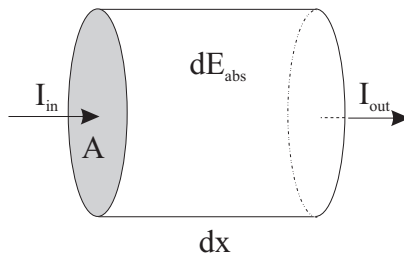$$\sigma(\omega_{kl}) = \frac{P(\omega_{kl})}{I(\omega_{kl})}. \tag{26}$$

FIG. 6. Cylindrical region of space through which a beam passes. The absorption in this region equals the difference between the flux entering and leaving the region.

Finally by combining equations 24 to 26, we see that the absorption cross-section is related to the transition dipole moment in the following manner

$$\sigma(\omega_{kl}) = \frac{\pi \omega_{kl}}{3\hbar c \epsilon_0} \mu_{kl}^2. \tag{27}$$

We remark that the cross section is a quantity that is averaged over all molecular orientations, whereas the transition dipole moment is linked to the molecular frame. We would now like to relate the power absorbed by a single molecule to the attenuation of the light because this is a quantity that can be straightforwardly determined. For this purpose we consider

13

a volume V through which a beam of light propagates (figure 6). This volume contains absorbing molecules at a concentration C and has a cross-sectional area A. The amount of energy (dE_{abs}) that is absorbed in this volume during the time dt is given by

$$dE_{\mathrm{abs}}(\omega_{kl}) = P_{\mathrm{tot}}(\omega_{kl})\,dt, \tag{28}$$

$$= CV\sigma(\omega_{kl})I(\omega_{kl})\,dt, \tag{29}$$

$$= C\sigma(\omega_{kl})I(\omega_{kl})A\,dx\,dt. \tag{30}$$

In the upper equation P_{tot} stands for the power absorbed by all molecules in the volume; in the second equation we have used eqn. 26 and the fact that the number of molecules in the volume is given by CV. dE_{abs} can also be obtained by considering the incoming and outgoing intensities (figure 6)

$$dE_{\mathrm{abs}}(\omega_{kl}) = (I_{\mathrm{in}}(\omega_{kl}) - I_{\mathrm{out}}(\omega_{kl}))A\,dt, \tag{31}$$

$$= -A\,dI\,dt. \tag{32}$$

Equating these two we obtain

$$dI(\omega_{kl}) = -\sigma(\omega_{kl})CI(\omega_{kl})\,dx. \tag{33}$$

This is Lambert-Beer's law in differential form; integration leads to the familiar result

$$T(\omega_{kl}) = \frac{I(\omega_{kl})}{I_0(\omega_{kl})} = e^{-\sigma(\omega_{kl})Cl}, \tag{34}$$

where I_0 is the light intensity before the entering the sample, T is the transmission and l is the sample length. In general one works with the absorbance, which is the natural logarithm of the transmission and has the advantage that it depends linearly on all parameters

$$\alpha(\omega_{kl}) = -\ln(T(\omega_{kl})) = \sigma(\omega_{kl})Cl. \tag{35}$$

Lambert-Beer's law provides the connection between the absorption cross section, which is a molecular property, and the attenuation of a beam of light, which can be easily determined experimentally.

V. MAXWELL-BLOCH EQUATIONS AND POLARITONS

A. Two-level system

in many spectroscopic techniques the studied material properties are related to those of atoms and molecules, which implies that the response of the systems should be described quantum-mechanically. Here we will derive the expression for the dielectric response of a two-level system. Starting point of the description of the dynamics of these systems and their interaction with the light field is the time-dependent Schrödinger equation:

$$(H_{sys} + H_{em}) \Psi(t) = i\hbar \frac{\partial \Psi}{\partial t}, \tag{36}$$

with H_{sys} the Hamiltonian of the system, $\Psi(t)$ the time-dependent wavefunction and H_{em} the Hamiltonian expressing the coupling of the system with the electro-magnetic field. In the electric-dipole approximation the Hamiltonian H_{em} equals $e \sum_n r_n E(t) \cos(\omega t)$ with e the elementary charge, r_n the position operator of the n-th electron, E(t) the envelope function of the electric field of the light and ω the frequency of the light.

For a two-level system the electromagnetic field can induce a transition between the two eigenstates of H_{sys} with wavefunctions ϕ_0 and ϕ_1 ($H_{sys}\phi_0 = \hbar\omega_0\phi_0$ and $H_{sys}\phi_1 = \hbar\omega_1\phi_1$). The time dependent wavefunction $\Psi(t)$ can then be written as :

$$\Psi(t) = C_0(t)\psi_0(t) + C_1(t)\psi_1(t) \tag{37}$$

with $\psi_j(t) = \phi_j e^{-i\omega_j t}$. Substitution of this equation in the time dependent Schrödinger equation gives :

$$H_{em} (C_0(t)\psi_0(t) + C_1(t)\psi_1(t)) = i\hbar \left(\frac{\partial C_0(t)}{\partial t}\psi_0(t) + \frac{\partial C_1(t)}{\partial t}\psi_1(t) \right) \tag{38}$$

We define $V_{10} = (eE/\hbar)\mu_{10}$ with $\mu_{10} = \langle \phi_1 | \sum_n r_n | \phi_0 \rangle$. Multiplication of both sides of equation (38) with ψ_0^* and integration over space yields :

$$V_{10}^* \cos \omega t e^{-i\omega_{01} t} C_1 = i \frac{\partial C_0}{\partial t} \tag{39}$$

with ω_{01} equal to $\omega_1 - \omega_0$. Here we used that $\int dr \psi_1^* \psi_1 = 1$ and $\int dr \psi_1^* \psi_0 = 0$ Similarly, multiplication of both sides of equation (38) with ψ_1^* and integration over space yields:

$$V_{10} \cos \omega t e^{i\omega_{01}t} C_0 = i\frac{\partial C_1}{\partial t} \tag{40}$$

The dynamics of the system that results from the interaction with light is thus fully expressed in the time dependence of the coefficients $C_0(t)$ and $C_1(t)$. As will be shown later, it is useful to express the dynamics of these coefficients in terms of so-called Bloch density matrix element ρ_{ij}. This matrix element is defined as $C_i C_j^*$. When we substitute $\widetilde{\rho_{10}} e^{i(\omega_0 - \omega)t}$ for ρ_{10} and we neglect the rapidly oscillating terms (rotating-wave approximation) we obtain the following equations for the density matrix elements :

$$\frac{\partial \widetilde{\rho_{10}}}{\partial t} = \frac{\partial \widetilde{\rho_{01}^*}}{\partial t} = -\frac{i}{2} V_{10}(\rho_{00} - \rho_{11}) - i(\omega_{01} - \omega)\widetilde{\rho_{10}} \tag{41}$$

$$\frac{\partial \rho_{11}}{\partial t} = -\frac{\partial \rho_{00}}{\partial t} = \frac{i}{2} \left(V_{01}\widetilde{\rho_{10}} - V_{10}\widetilde{\rho_{01}} \right) \tag{42}$$

The polarization $\mathcal{P}$ of a two level system is given by $\mathcal{P} = -Ne\{\mu_{10}\rho_{10}e^{-i\omega_{01}t} + c.c.\}$ and $\mathcal{P}$ is equal to $\frac{1}{2}\{Pe^{-i\omega t} + c.c.\}$. The envelope function $P(t)$ is equal to $-2Ne\mu_1\widetilde{\rho_{10}}$. Using this equality and setting $n = \rho_{11} = 1 - \rho_{00}$ we obtain the Bloch equations for the polarization and the population of the upper state :

$$\frac{\partial P}{\partial t} = \frac{iNe^2|\mu_{01}|^2}{\hbar} E(1 - 2n) + i(\omega - \omega_0)P \tag{43}$$

$$\frac{\partial n}{\partial t} = \frac{i}{4\hbar N} \left(EP^* - E^*P \right) \tag{44}$$

Adding relaxation terms:

$$\frac{\partial P}{\partial t} = \frac{iNe^2|\mu_{01}|^2}{\hbar} E(1 - 2n) + i(\omega - \omega_0)P - \frac{P}{T_2} \tag{45}$$

$$\frac{\partial n}{\partial t} = \frac{i}{4\hbar N} \left(EP^* - E^*P \right) - \frac{n}{T_1} \tag{46}$$

The (nonlinear effects) of the coupling of light with a two-level system can be described by these two equations in combination with the wave equation.

In the case of linear response, the change in the population can be neglected which implies that the two equations for the polarization and the population are decoupled. The

equation for the polarization can easily be solved in the frequency domain. This means that we write $E(t) = (1/2) \int d\omega' E(\omega') e^{-i(\omega')t} + c.c.\}$. The same can be done for the polarization: $P(t) = (1/2) \int d\omega' P(\omega') e^{-i(\omega')t} + c.c.\}$. Substitution of these expressions for P and E in the equation for $P(t)$ yields:

$$-\int d\omega' e^{-i(\omega')t} i\omega' P(\omega') = \frac{iNe^2|\mu_{01}|^2}{\hbar} E(\omega')(1 - 2n_0) + \tag{47}$$

$$i(\omega - \omega_{01})P(\omega') - \frac{P(\omega')}{T_2} \tag{48}$$

This equation can be solved for each frequency component separately. If we redefine $\omega = \omega + \omega'$ and define $P(\omega) = \chi(\omega)E(\omega)$, we obtain:

$$\chi(\omega) = \frac{Ne^2|\mu_{01}|^2}{\hbar} \frac{1}{\omega_{01} - \omega - i\gamma} \tag{49}$$

Separating the real and imaginary parts, the response of the two-level system can be written as:

$$\chi(\omega) = \frac{Ne^2|\mu_{01}|^2}{\hbar} \left\{ \frac{1}{\omega_{01} - \omega - i\gamma} \right\} = \frac{Ne^2|\mu_{01}|^2}{\hbar} \left\{ \frac{(\omega_{01} - \omega)}{(\omega_{01} - \omega)^2 + \gamma^2} + \frac{i\gamma}{(\omega_{01} - \omega)^2 + \gamma^2} \right\} \tag{50}$$

The imaginary part of this response represents a Lorentzian with central frequency ω_0 and width 2γ.

B. Polaritons

From Maxwell's equation for a dielectric the so-called wave equation can be derived:

$$\left(\frac{\partial^2}{\partial x^2} + \frac{\partial^2}{\partial y^2} + \frac{\partial^2}{\partial z^2} \right) \mathcal{E} = \frac{1}{\epsilon_0 c^2} \left(\frac{\partial^2 \epsilon_0 \mathcal{E}}{\partial t^2} + \frac{\partial^2 \mathcal{P}}{\partial t^2} \right) \tag{51}$$

The function $\mathcal{E}(r,t)$ can be expressed as a sum of plane waves: $\mathcal{E}(r,t) = (1/2) \int d\omega \{ E(\omega) e^{ik(\omega)r - i(\omega)t} + c.c.\}$. In this expression the r dependence of the field is contained in the sum over $e^{ik(\omega)r}$, where $k(\omega)$ represents the wave vector depending on the frequency ω. The same can be done for the polarization $\mathcal{P}(r,t) = (1/2) \int d\omega \{ P(\omega) e^{ik(\omega)r - i(\omega)t} + c.c.\}$. If we substitute these expressions for $\mathcal{E}(r,t)$ and $\mathcal{P}(r,t)$ in the wave equation, we obtain:

$$k^2(\omega)E(\omega)e^{ik(\omega)r-i(\omega)t} = \frac{1}{\epsilon_0 c^2}\left(\omega^2\epsilon_0 E(\omega)e^{ik(\omega)z-i(\omega)t} + \omega^2 P(\omega)e^{ik(\omega)z-i(\omega)t}\right) \tag{52}$$

Substitution of $P(\omega) = \epsilon_0\chi^{(1)}(\omega)E(\omega)$ in the wave equation gives a relation between the wave vector k and the frequency ω for each frequency component:

$$k^2 = \frac{\omega^2(1+\chi^{(1)}(\omega))}{c^2}. \tag{53}$$

The wave vector is a complex quantity and can be written as $k = (\omega/c)[n(\omega)+i\kappa(\omega)]$. The parameter $n(\omega)$ is denoted as the refractive index and determines the phase velocity of light: $v_\mathrm{p} = c/n$. The parameter $\kappa(\omega)$ represents the damping of the light wave in the medium: $e^{ik(\omega)r} = e^{i\omega n(\omega)/c}e^{-\omega\kappa(\omega)/c}$. Hence, the light shows a simple exponential damping as a function of r for each frequency. The parameter κ is related in a very simple manner to the decrease of the amplitude of light following the law of Lambert Beer:

$$I(z,\omega) = I(0,\omega)e^{-\alpha z}. \tag{54}$$

It follows that the absorption coefficient α is equal to $2\omega\kappa(\omega)/c$. It should be noted that this does not mean that a light pulse propagating through a medium would only show a change (decrease) of its amplitude and not of its shape. The afore mentioned exponential damping of the amplitude applies to the light in the *frequency* domain. In the time domain the propagation of light through a medium can lead to very complicated interference effects and thus to a strong distortion of the original shape of the light pulse.

The parameters n and κ are related to the real and imaginary part of the dielectric susceptibilty in the following way:

$$n^2(\omega) - \kappa^2(\omega) = 1 + \chi^{(1)}_{\mathrm{re}}(\omega) \tag{55}$$

$$2n\kappa = \chi^{(1)}_{\mathrm{im}}(\omega) \tag{56}$$

The decomposition of the light field in plane waves $e^{ik(\omega)r-i(\omega)t}$ is a powerful method to calculate the change of the shape of a light pulse upon propagation. For instance, at $r = 0$: $\mathcal{E}(r=0,t) = \frac{1}{2}\{\int E(\omega)e^{-i(\omega)t}d\omega + c.c.\}$, while at $r = l$: $\mathcal{E}(r=l,t) = \frac{1}{2}\{\int E(\omega)e^{ik(\omega)l-i(\omega)t}d\omega +$

18

c.c.}. Hence, the change of the shape of the light pulse upon propagation from $z = 0$ to $z = l$ can be obtained by taking the Fourier transform $\int d\omega e^{i\omega t}\mathcal{E}(0,t)$ (yielding the Fourier components $E(\omega)$, multiplying each of these components with $e^{ik\omega l}$, and taking the Fourier transform $\int d\omega e^{-i\omega t}E(\omega)e^{ik\omega l}$ back to the time domain yielding $\mathcal{E}(l,t)$. In a single equation:

$$\mathcal{E}(l,t) = \int d\omega e^{ik(\omega)l - i\omega t} \int dt e^{i\omega t}\mathcal{E}(0,t) \tag{57}$$

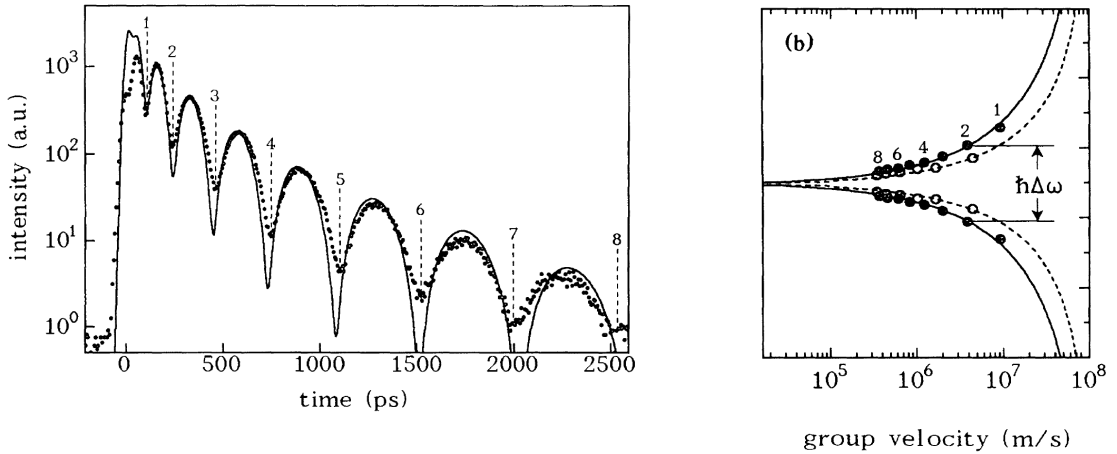The effects of propagation are illustrated in Figure 7.

FIG. 7. Effect of polariton propagation near the resonance with the 1S exciton transition in a Cu$_2$O crystal. The light pulse has an initial pulse duration of 30 ps. The points are experimental results and the curves are calculated using equation (57). Figure b shows the frequency of the light components as a function of the group velocity. (After D. Forster et al., Phys. Rev. Lett. **67**, 2343 (1991))

It is clearly seen in this figure that frequency components close to a resonance propagate much slower and leave the sample much later than the frequency components that are far away from the resonance.

The coupled equations for the polarization and the wave equation can also be solved in the time domain:

$$\mathcal{E}(r,t) = \mathcal{E}_0(t - r/v) - \frac{bx}{2}\int_{-\infty}^{t-x/v} dt' e^{[(1/T_2) - i\Delta\omega][t'-t]}\mathcal{E}_0(t')\frac{J_1\{[bx(t-t')]^{1/2}\}}{[bx(t-t')]^{1/2}}, \tag{58}$$

19

where J_1 denotes the Bessel function of first order. This equation holds for any pulse shape entering the sample at $x = 0$. The factor b contains several material parameters $b = 2\alpha/T_2 = 8\pi\omega Ne^2|\mu_{12}|^2/c\hbar$, where α denotes the absorption coefficient at the maximum of the absorption band.

It should be noted that the obtained solution for $\mathcal{E}(l, t)$ is only a correct solution of the Maxwell wave equation if the polarization depends linearly on the electric field. If the polarization contains terms that are nonlinear in the electric field, the right-hand side of the transformed wave equation of equation (56) contains additional terms. These additional terms will give rise to modifications of the propagated light pulse and can give rise to the generation of new light fields.

VI. VIBRATIONAL SATURATION SPECTROSCOPY

A. Nonlinear optics in general

For strong light fields the response of the material acquires non-linear components in the electric field of the light:

$$\mathcal{P} = \chi^{(1)}\mathcal{E} + \chi^{(2)}\mathcal{E}^2 + \chi^{(3)}\mathcal{E}^3 + \cdots = \chi^1\mathcal{E} + \mathcal{P}_{\mathrm{NL}}, \tag{59}$$

with $\mathcal{P}$ the polarization (=induced dipole per volume) of the medium and $\mathcal{E}$ the electric field of light.

Other definition for nonlinear optics: light changes the response for light. Is this possible for a harmonic oscillator? For example a light pulse excites 100% from $v = 0$ to $v = 1$. Absorption of $v = 0 \rightarrow 1$ before the excitation:

$$B_{0\rightarrow 1} \sim |\langle\phi_1|x|\phi_0\rangle|^2 = 1 \tag{60}$$

after excitation:

$$B_{1\rightarrow 2} \sim |\langle\phi_2|x|\phi_1\rangle|^2 = 2 \tag{61}$$

However, there is also stimulated emission:

$$B_{1\to0} \sim -|\langle\phi_1|x|\phi_0\rangle|^2 = -1 \tag{62}$$

$$B_{1\to2} + B_{1\to0} = B_{0\to1} \tag{63}$$

In general, the absorption $B_{n\to n+1} \sim n+1$ while the stimulated emission equals $B_{n\to n-1} \sim n$. Hence, irrespective how the population is distributed over the different levels of the harmonic oscillator, the net absorption (difference between absorption and emission) is always the same. Clearly, this is no longer the case if the frequency spacing between the levels is not constant: anharmonic oscillator. In that case the stimulated emission can no longer be subtracted from the absorption. Hence, to acquire nonzero χ^2, χ^3, the resonances of the medium (= electronic transitions, vibrations, rotations) should be *anharmonic.*

An example of an extremely anharmonic system is the two-level system. If 50% of the population is excited to $v = 1$ in a two-level system: the absorption is given by $B_{0\to1} \sim |\langle\phi_1|x|\phi_0\rangle|^2$, while the stimulated emission equals $B_{1\to0} \sim -|\langle\phi_1|x|\phi_0\rangle|^2$. There clearly is no absorption from $v = 1$ as the system only contains two levels. Hence, the total absorption is: $B_{0\to1} + B_{1\to0} = 0$. The medium has thus become completely transparent

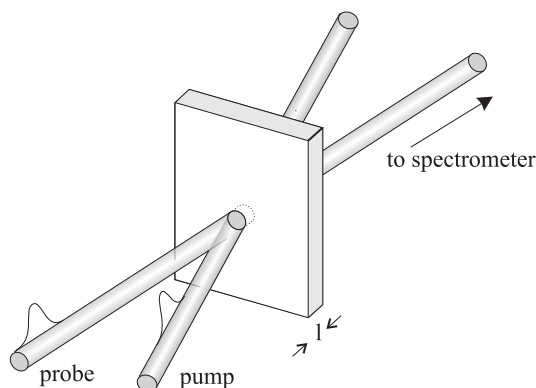## B. Vibrational pump-probe spectroscopy

FIG. 8. Schematic representation of the pump-probe experiment. A sample of thickness l is illuminated by a pump pulse, which excites a significant fraction of the molecules. Next a time-delayed probe pulse is used to monitor the spectral changes induced by the first pulse.

Up to now we have mainly dealt with linear absorption, which provides information about the *static* properties of molecules. In some cases *dynamical* information can also be obtained from a linear spectrum. This is because the spectral widths of transitions contain information about the equilibrium fluctuations experienced by molecules. However, often there are additional (inhomogeneous) broadening mechanisms at play which obscure the dynamical information contained in the absorption lineshape. Nonlinear spectroscopies, such as pump-probe spectroscopy, overcome this problem by directly probing non-equilibrium properties of a sample. In particular, the sample is first brought into a non-equilibrium state by an intense pump pulse, after which the relaxation to the equilibrium state is monitored by a weak, time-delayed probe pulse (figure 8).

Here we will discuss the general principles that underlie the pump-probe experiment, focusing in particular on those aspects that are observed in the vibrational pump-probe spectroscopy of water. We first consider the absorption α_0 experienced by a weak probe pulse in the absence of a pump pulse

$$\alpha_0(\omega) = \sigma_{01}(\omega)Cl, \tag{64}$$

$$= \sigma_{01}(\omega)n, \tag{65}$$

where we have introduced the symbol n to denote the concentration per unit surface. After excitation by the pump pulse the sample will exhibit a modified absorption due to three effects (figure 9). First, after excitation there are less molecules in the ground state, so that the sample shows a decreased absorption at the fundamental frequency. A second effect leading to a decreased absorption at this frequency is stimulated emission from the excited state. Finally, the excited molecules can be further excited to the $v = 2$ state, which causes an increased absorption at the frequency of the $1 \rightarrow 2$ transition. These effects lead to the following expression for the absorption

$$\alpha(\omega) = \sigma_{01}(\omega)(n - 2N_1) + \sigma_{12}(\omega)N_1, \tag{66}$$

where N_1 is the concentration of excited molecules. The factor 2 enters because ground state depletion and stimulated emission contribute equally to the absorption change. In a

pump-probe experiment we usually record the absorption spectrum of the probe beam in the presence and absence of the pump pulse. The transient absorption $\Delta\alpha$ is defined as the difference between these two spectra

$$\Delta\alpha(\omega) = \alpha(\omega) - \alpha_0(\omega) = (-2\sigma_{01}(\omega) + \sigma_{12}(\omega))N_1. \tag{67}$$
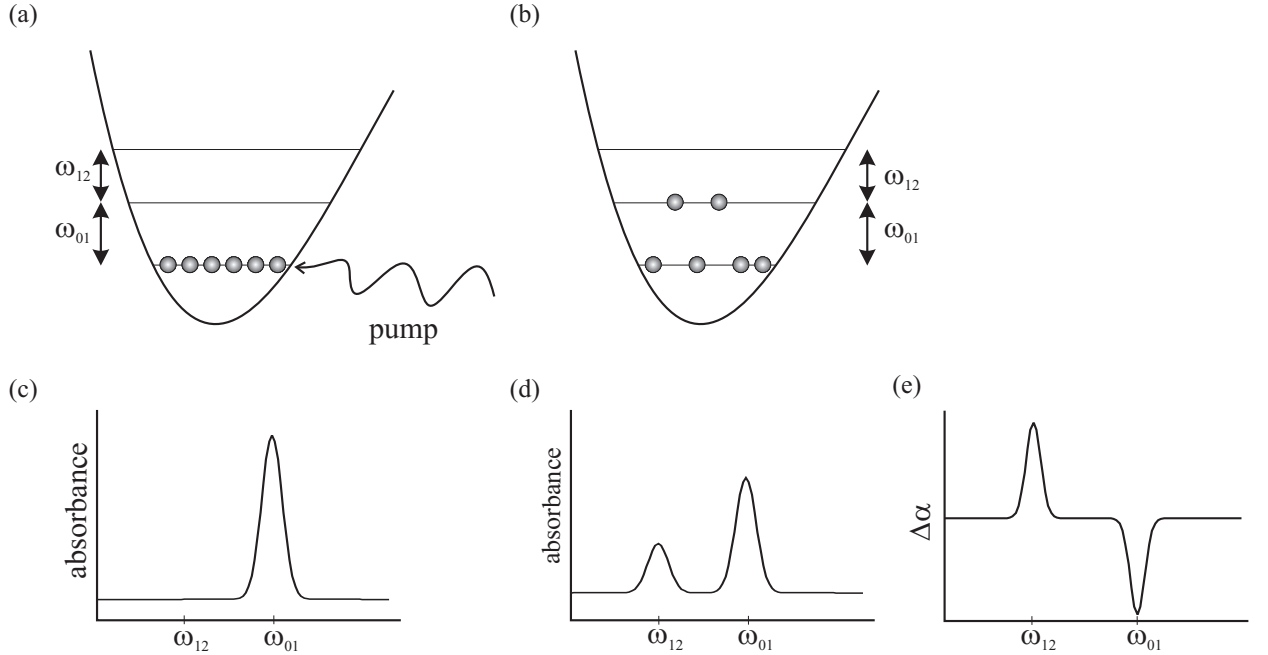

FIG. 9. Principle of vibrational pump-probe spectroscopy. a,c) Potential energy diagram of a typical vibration. In thermal equilibrium all molecules are in the ground state, which leads to an absorption at ω_{01}. b,d) A pump pulse promotes a significant fraction of the molecules to the first excited state. This leads to a decreased absorption at ω_{01} and an increased absorption at ω_{12}. e) The transient spectrum is the difference between the spectra in the presence and absence of the pump pulse.

The transient spectrum consists of two contributions; the negative contribution, arising from the ground state depletion and stimulated emission, is called the bleaching signal; the positive contribution is called the induced absorption or excited state absorption.
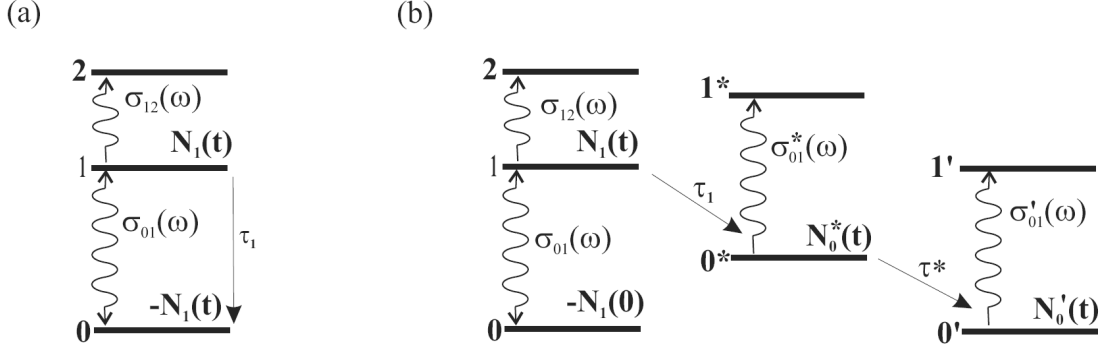
23

C. Vibrational relaxation

FIG. 10. a) Example of a relaxation mechanism in which an excited vibration relaxes directly to the ground state. b) Example of a relaxation mechanism that involves an intermediate state. In this example the molecules do not relax to the original ground state. This accounts for an irreversible change induced by the pump pulse, such as a chemical reaction or sample heating. In this figure wiggly lines denote radiative transitions, while the arrows represent non-radiative transitions.

After excitation the transient spectrum will decay because excited molecules relax to the ground state. In general the excited state population decays exponentially with time. If relaxation proceeds immediately to the ground state (figure 10a) this leads to an exponential decay of both the induced absorption and the bleach,

$$\Delta\alpha(\omega, t) = (-2\sigma_{01}(\omega) + \sigma_{12}(\omega))N_1(t), \tag{68}$$

$$= (-2\sigma_{01}(\omega) + \sigma_{12}(\omega))N_1(0)e^{-t/\tau_1}, \tag{69}$$

where τ_1 is the lifetime of the vibration. The lifetime of a vibration depends strongly on its surroundings; in solution it can vary from hundreds of picoseconds to less than a picosecond. For example, the vibrational lifetime of the OD vibration of HDO in H_2O is 1.8 ± 0.2 ps, while the surface OD groups of deuterated zeolites can have lifetimes of 70 ps.

In general vibrational relaxation proceeds through complicated mechanisms that may involve a number of intermediate states. An example is shown in figure 10b. Here the

intermediate levels represent states in which the original vibration has relaxed and excited a low-frequency inter- or intramolecular vibration. If the two vibrations are coupled via an anharmonic interaction, excitation of the low-frequency mode will result in a frequency shift of the high-frequency vibration. Figure 11 illustrates this effect for the H_2O molecule. We will describe this effect by assigning different spectra to the intermediate states than to the excited state. The relaxation mechanism in figure 10b also shows that excited molecules do not necessarily relax to the original ground state. This is a way of describing irreversible changes induced by the pump pulse. For pump pulses in the visible or ultraviolet the irreversible change often consists in a chemical reaction. In the infrared it is generally only heating of the sample, although a few examples of infrared-induced chemical reactions are known. For the relaxation mechanism shown in figure 10b we can write the following expression for the transient signal

$$\Delta\alpha(\omega, t) = \sigma_{12}(\omega)N_1(t) - \sigma_{01}N_1(0) - \sigma_{01}(\omega)N_1(t)$$
$$+\sigma_{01}^*(\omega)N_0^*(t) + \sigma_{01}'(\omega)N_0'(t), \tag{70}$$

where $\sigma_{01}^*(\omega)$ and $\sigma_{01}'(\omega)$ represent the cross section spectra of the intermediate state and of the modified ground state. The expression consists of five terms. The first term represents the excited state absorption. The second and third term arise from ground state depletion and stimulated emission, respectively. Finally the fourth and the fifth term are due to the absorption of the intermediate state and the modified ground state.
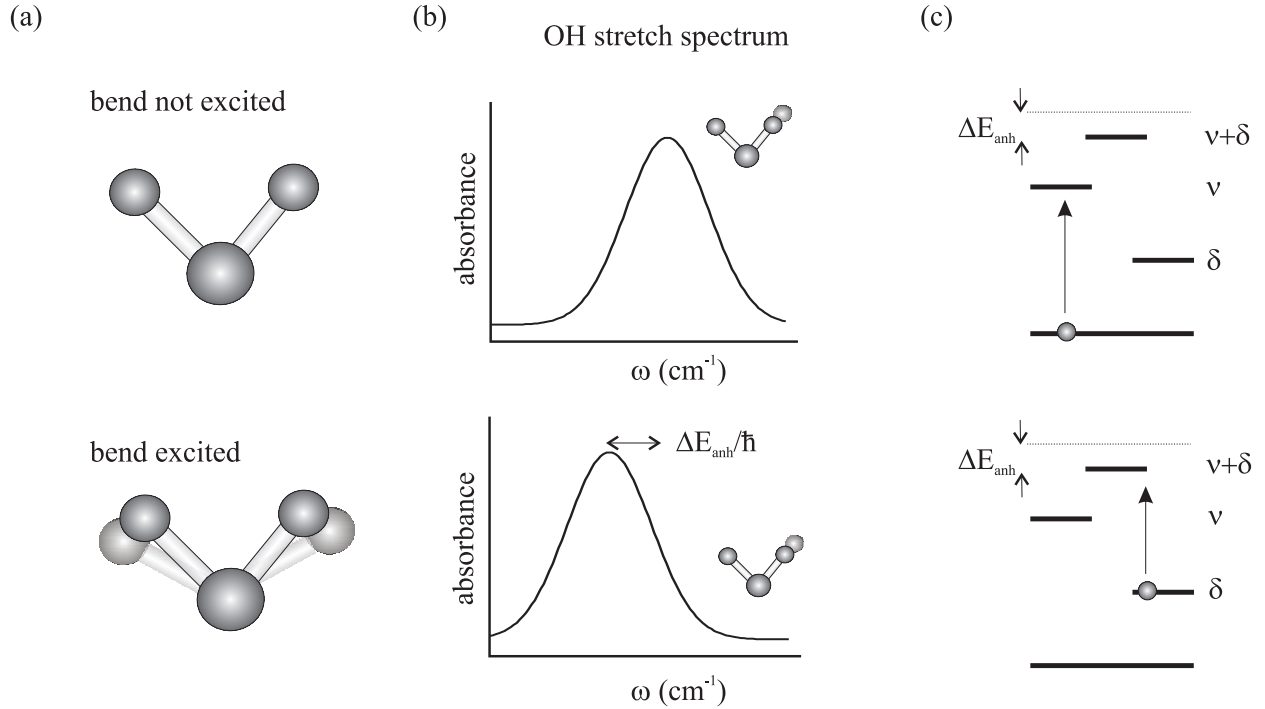
FIG. 11. Effect of the anharmonic interaction between the OH stretching vibration (ν) and the bending vibration (δ) of H_2O. a) An H_2O molecule in its vibrational ground state and an H_2O molecule with one excitation quantum in the bending vibration. b) Absorption spectrum of the OH-stretching vibration of H_2O for the vibrational ground state and for the first excited state of the bending vibration. The OH stretching spectrum shifts to lower frequencies if the bending vibration is excited. c) Energy level diagram of H_2O taking into account only the first excited states of the stretching (ν) and bending vibrations (δ). Due to the anharmonic interaction (ΔE_{anh}) the doubly excited state lies lower in energy than the sum of the two singly excited states.

VII. RIGOROUS: NONLINEAR COUPLING OF LIGHT TO A TWO-LEVEL SYSTEM

The nonlinear interaction between light and material resonances can often be described in a perturbative approach. Starting point for this approach are the Bloch equations for a two-level system of the last chapter. We will in this case use the rotating wave approximation. In addition we will use the notation $\rho_{10}^{(n)}$ for $\widetilde{\rho_{10}^{(n)}}$. The subsequent orders in the electric field can be generated as follows:

$$\frac{\partial \rho_{10}^{(n+1)}}{\partial t} = -\frac{ieE\mu_{10}}{2\hbar}(\rho_{00}^{(n)} - \rho_{11}^{(n)}) - \left\{i(\omega_{01} - \omega) + \frac{1}{T_{2_{0\to1}}}\right\}\rho_{10}^{(n+1)} \tag{71}$$

$$\frac{\partial \rho_{11}^{(n+1)}}{\partial t} = -\frac{\partial \rho_{00}^{(n+1)}}{\partial t} = \frac{ieE^*\mu_{01}}{2\hbar}\rho_{10}^{(n)} - \frac{ieE\mu_{10}}{2\hbar}\rho_{01}^{(n)} \tag{72}$$

In these equations the superscript (n) denotes the order in the electric field. Before the interaction with the light field there is in general no coherence present for the ensemble. Hence, $\rho_{01}^{(0)} = \rho_{10}^{(0)} = 0$. The initial population difference between the levels 1 and 2 will in general not be equal to zero: $\rho_{00}^{(0)} - \rho_{11}^{(0)} \neq 0$. The electric field E represents the total electric field. This field can thus be formed by the sum of different light pulses applied to the system.

In many experiments, the generated signal results from a polarization that is of third-order in the electric field. Examples are saturation spectroscopy and photon-echo spectroscopy. The third-order polarization is proportional to the off-diagonal density matrix elements $\rho_{10}^{(3)}$ and $\rho_{01}^{(3)}$. For $\rho_{10}^{(3)}$ we have:

$$\rho_{10}^{(3)}(t) = -\frac{i\mu_{10}}{2\hbar}\int_{-\infty}^{t} dt_1 E(t_1)(\rho_{00}^{(2)}(t_1) - \rho_{11}^{(2)}(t_1))R(t - t_1) \tag{73}$$

This equation implies that the value of $\rho_{10}^{(3)}$ at time t is the sum of the products of the electric field and the diagonal density matrix element $\rho_D^{(2)}$ over all previous times t_1. In addition, each of these contributions to $\rho_{10}^{(3)}$ can show relaxation in the time interval between its time of generation t_1 and the time t. In addition the relative phase of these contributions will evolve depending on the frequency difference between the generating electric field and the resonance frequency. The relaxation and phase evolution are expressed by the function $R(t - t_1)$. In case the relaxation can be described with a single time constant $T_{2_{0\to1}}$:

$$R(t - t_1) = e^{-i(\omega - \omega_{01})(t - t_1)}e^{(t - t_1)/T_{2_{0\to1}}}. \tag{74}$$

For the diagonal matrix element $\rho_{11}^{(2)}$ a similar equation applies. Hence:

$$\rho_{11}^{(2)}(t) = \frac{i\mu_{01}}{2\hbar}\left\{\int_{-\infty}^{t} dt_1 E^*(t_1)\rho_{10}^{(1)}(t_1) + E(t_1)\rho_{01}^{(1)}(t_1)\right\}P(t - t_1), \tag{75}$$

with $P(t_1 - t_2)$ a population relaxation function:

$$P(t - t_1) = e^{(t-t_1)/T_1}. \tag{76}$$

Similar:

$$\rho_{00}^{(2)}(t) = -\frac{i\mu_{01}}{2\hbar} \left\{ \int_{-\infty}^{t} dt_1 E^*(t_1)\rho_{10}^{(1)}(t_1) + E(t_1)\rho_{01}^{(1)}(t_1) \right\} P(t - t_1). \tag{77}$$

Finally:

$$\rho_{10}^{(1)}(t) = -\frac{i\mu_{01}}{2\hbar} \int_{-\infty}^{t} dt_1 E(t_1)(\rho_{00}^{(0)} - \rho_{11}^{(0)})R(t - t_1) \tag{78}$$

Substitution of equation (78) and its complex conjugate in equations (75) and (77)for $\rho_{11}^{(2)}$ and $\rho_{00}^{(2)}$, and substitution of the latter equations in equation (73) yields in total four contributions to the third-order off-diagonal density matrix element $\rho_{10}^{(3)}$. These terms can be represented with so-called Feynman diagrams, as illustrated in Figure 12.
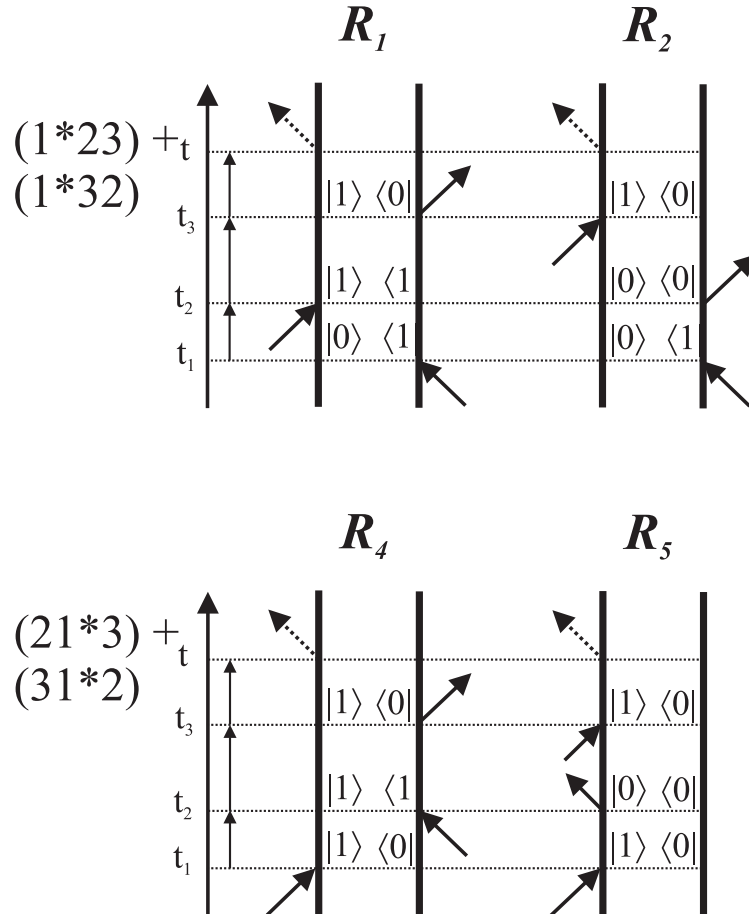

FIG. 12. Double-sided Feynman diagrams representing the field interactions and corresponding response functions to generate a third-order polarization in a two-level system.

The arrows in the Feynman diagram represent the field interactions, leading to a change in state of either the ket or the bra. An E field can either excite the ket or de-excite the bra, while an E^* field either generates a bra or destroys a ket. The states $|0\rangle$ and $\langle 0|$ can only be excited, while the states $|1\rangle$ and $\langle 1|$ (in a two-level system) can only be de-excited. The terms corresponding to $\rho_{11}^{(2)}$ and $\rho_{00}^{(2)}$ can be taken together, yielding the following expression for $\rho_{10}^{(3)}$:

$$\rho_{10}^{(3)}(t) = -i \left(2\frac{\mu_{01}}{2\hbar} \right)^3 \int_{-\infty}^{t} dt_1 \int_{-\infty}^{t_1} dt_2 \int_{-\infty}^{t_2} dt_3 \tag{79}$$
$$[E(t_1)E(t_2)E^*(t_3)R(t-t_1)P(t_1-t_2)R^*(t_2-t_3) +$$
$$E(t_1)E^*(t_2)E(t_3)R(t-t_1)P^*(t_1-t_2)R(t_2-t_3)]$$

The above equation is very general in nature. The different third-order signals that are generated can be distinguished by the directions (wave vectors) of the electric fields that constitute the total electric field E and the direction in which the generated signal is observed. For instance, in the case of pump-probe saturation spectroscopy, the electric field E consists of two fields with wave vectors k_{pu} and k_{pr} and the nonlinear signal in the direction of the probe is detected. However, simultaneously with this signal a signal in the direction $2k_{pu} - k_{pr}$ will be generated that can be independently detected.

VIII. BLOCH EQUATIONS FOR A THREE-LEVEL SYSTEM

The above formalism can be easily extended to a three-level system. In a three-level system the states $|1\rangle$ and $\langle 1|$ can be further excited to $|2\rangle$ and $\langle 2|$. In this section we will derive the expression for the dielectric response of a three-level system. Starting point of the description of the dynamics of these systems and their interaction with the light field is the time-dependent Schrödinger equation:

$$\left(H_{sys} + H_{em} \right) \Psi(t) = i\hbar \frac{\partial \Psi}{\partial t}, \tag{80}$$

with H_{sys} the Hamiltonian of the system, $\Psi(t)$ the time-dependent wavefunction and H_{em} the Hamiltonian expressing the coupling of the system with the electro-magnetic field. In

the electric-dipole approximation the Hamiltonian H_{em} equals $e \sum_n r_n E \cos(\omega t)$ with e the elementary charge, r_n the position operator of the n-th electron, E the amplitude of the electric field of the light and ω the frequency of the light.

For a three-level system the electromagnetic field can induce transitions between the three eigenstates of H_{sys} with wavefunctions ϕ_0, ϕ_1, and ϕ_2 ($H_{sys}\phi_j = \hbar\omega_j\phi_j$ with $j = 0, 1, 2$). The time dependent wavefunction $\Psi(t)$ can then be written as :

$$\Psi(t) = C_0(t)\psi_0(t) + C_1(t)\psi_1(t) + C_2(t)\psi_2(t) \tag{81}$$

with $\psi_j(t) = \phi_j e^{-i\omega_j t}$. Substitution of this equation in the time dependent Schrödinger equation gives :

$$H_{em}\left(C_0(t)\psi_0(t) + C_1(t)\psi_1(t) + C_3(t)\psi_3(t)\right) = i\hbar\left(\frac{\partial C_0(t)}{\partial t}\psi_0(t) + \frac{\partial C_1(t)}{\partial t}\psi_1(t) + \frac{\partial C_2(t)}{\partial t}\psi_2(t)\right) \tag{82}$$

Here we have used that $H_{sys}\phi_j = \hbar\omega_j\phi_j$ and that $i\hbar\frac{\partial\psi_j(t)}{\partial t} = \hbar\omega_j\psi_j(t)$. Succesive multiplication of both sides of this equation with ψ_j^* and integration over space yields :

$$i\hbar\frac{\partial C_0(t)}{\partial t} = C_0(t)H_{em,00}e^{-i\omega_0 t} + C_1(t)H_{em,01}e^{-i\omega_1 t} + C_2(t)H_{em,02}e^{-i\omega_2 t} \tag{83}$$

$$i\hbar\frac{\partial C_1(t)}{\partial t} = C_0(t)H_{em,10}e^{-i\omega_0 t} + C_1(t)H_{em,11}e^{-i\omega_1 t} + C_2(t)H_{em,12}e^{-i\omega_2 t} \tag{84}$$

$$i\hbar\frac{\partial C_2(t)}{\partial t} = C_0(t)H_{em,20}e^{-i\omega_0 t} + C_1(t)H_{em,21}e^{-i\omega_1 t} + C_2(t)H_{em,22}e^{-i\omega_2 t}, \tag{85}$$

with $H_{em,jk} = \langle\psi_j|H_{em}|\psi_k\rangle$. Using $H_{em} = e\sum_n r_n E_0 cos(\omega t)$, we define $V_{jk} = (eE_0\mu_{jk}/\hbar)$ with $\mu_{jk} = \langle\phi_j|\sum_n r_n|\phi_k\rangle$. If we assume that $\mu_{jj} = 0$ and we define $\omega_{01} = \omega_1 - \omega_0$, $\omega_{02} = \omega_2 - \omega_0$, and $\omega_{12} = \omega_2 - \omega_1$, we obtain:

$$i\frac{\partial C_0(t)}{\partial t} = C_1(t)V_{01}cos(\omega t)e^{-i\omega_{01}t} + C_2(t)V_{02}cos(\omega t)e^{-i\omega_{02}t} \tag{86}$$

$$i\frac{\partial C_1(t)}{\partial t} = C_0(t)V_{10}cos(\omega t)e^{i\omega_{01}t} + C_2(t)V_{12}cos(\omega t)e^{-i\omega_{12}t} \tag{87}$$

$$i\frac{\partial C_2(t)}{\partial t} = C_0(t)V_{20}cos(\omega t)e^{i\omega_{02}t} + C_1(t)V_{21}cos(\omega t)e^{i\omega_{12}t} \tag{88}$$

We use the above equations to derive expressions for the density matrix elements $\rho_{jk} = C_jC_k^*$:

$$\frac{\partial \rho_{jk}}{\partial t} = C_j \frac{\partial C_k^*}{\partial t} + \frac{\partial C_j}{\partial t} C_k^* \tag{89}$$

It follows that:

$$\frac{\partial \rho_{00}}{\partial t} = i\cos(\omega t) \left\{ \rho_{01} V_{10} e^{i(\omega_1 - \omega_0)t} + \rho_{02} V_{20} e^{i(\omega_2 - \omega_0)t} - \rho_{10} V_{01} e^{-i(\omega_1 - \omega_0)t} - \rho_{20} V_{02} e^{-i(\omega_2 - \omega_0)t} \right\} \tag{90}$$

$$\frac{\partial \rho_{11}}{\partial t} = i\cos(\omega t) \left\{ \rho_{10} V_{01} e^{i(\omega_0 - \omega_1)t} + \rho_{12} V_{21} e^{i(\omega_2 - \omega_1)t} - \rho_{01} V_{10} e^{-i(\omega_0 - \omega_1)t} - \rho_{21} V_{12} e^{-i(\omega_2 - \omega_1)t} \right\} \tag{91}$$

$$\frac{\partial \rho_{22}}{\partial t} = i\cos(\omega t) \left\{ \rho_{20} V_{02} e^{i(\omega_0 - \omega_2)t} + \rho_{21} V_{12} e^{i(\omega_1 - \omega_2)t} - \rho_{02} V_{20} e^{-i(\omega_0 - \omega_2)t} - \rho_{12} V_{21} e^{-i(\omega_1 - \omega_2)t} \right\} \tag{92}$$

$$\frac{\partial \rho_{10}}{\partial t} = -i\cos(\omega t) \left\{ V_{10}(\rho_{00} - \rho_{11}) e^{i(\omega_1 - \omega_0)t} - V_{20}\rho_{12} e^{i(\omega_2 - \omega_0)t} - V_{12}\rho_{20} e^{i(\omega_1 - \omega_2)t} \right\} \tag{93}$$

$$\frac{\partial \rho_{20}}{\partial t} = -i\cos(\omega t) \left\{ V_{20}(\rho_{00} - \rho_{22}) e^{i(\omega_2 - \omega_0)t} - V_{10}\rho_{21} e^{i(\omega_1 - \omega_0)t} - V_{21}\rho_{10} e^{i(\omega_2 - \omega_1)t} \right\} \tag{94}$$

$$\frac{\partial \rho_{21}}{\partial t} = -i\cos(\omega t) \left\{ V_{21}(\rho_{11} - \rho_{22}) e^{i(\omega_2 - \omega_1)t} - V_{01}\rho_{20} e^{i(\omega_0 - \omega_1)t} - V_{20}\rho_{01} e^{i(\omega_2 - \omega_0)t} \right\} \tag{95}$$

When we substitute ρ_{10} by $\widetilde{\rho_{10}} e^{i(\omega_1 - \omega_0 - \omega)t}$, ρ_{21} by $\widetilde{\rho_{21}} e^{i(\omega_2 - \omega_1 - \omega)t}$, ρ_{20} by $\widetilde{\rho_{20}} e^{i(\omega_2 - \omega_0 - 2\omega)t}$, and if we use the rotating wave approximation, the above equations become:

$$\frac{\partial \rho_{00}}{\partial t} = \frac{i}{2} \left\{ \widetilde{\rho_{01}} V_{10} + \rho_{02} V_{20} e^{i\omega t} - \widetilde{\rho_{10}} V_{01} - \rho_{20} V_{02} e^{-i\omega t} \right\} \tag{96}$$

$$\frac{\partial \rho_{11}}{\partial t} = \frac{i}{2} \left\{ \widetilde{\rho_{10}} V_{01} + \widetilde{\rho_{12}} V_{21} - \widetilde{\rho_{01}} V_{10} - \widetilde{\rho_{21}} V_{12} \right\} \tag{97}$$

$$\frac{\partial \rho_{22}}{\partial t} = \frac{i}{2} \left\{ \widetilde{\rho_{20}} V_{02} e^{-i\omega t} + \widetilde{\rho_{21}} V_{12} - \widetilde{\rho_{02}} V_{20} e^{i\omega t} - \widetilde{\rho_{12}} V_{21} \right\} \tag{98}$$

$$\frac{\partial \widetilde{\rho_{10}}}{\partial t} = -\frac{i}{2} \left\{ V_{10}(\rho_{00} - \rho_{11}) - V_{20}\widetilde{\rho_{12}} e^{i\omega t} - V_{12}\widetilde{\rho_{20}} - i(\omega_1 - \omega_0 - \omega)\widetilde{\rho_{10}} \right\} \tag{99}$$

$$\frac{\partial \widetilde{\rho_{20}}}{\partial t} = -\frac{i}{2} \left\{ V_{20}(\rho_{00} - \rho_{22}) e^{i\omega t} - V_{10}\widetilde{\rho_{21}} - V_{21}\widetilde{\rho_{10}} - i(\omega_2 - \omega_0 - 2\omega)\widetilde{\rho_{20}} \right\} \tag{100}$$

$$\frac{\partial \widetilde{\rho_{21}}}{\partial t} = -\frac{i}{2} \left\{ V_{21}(\rho_{11} - \rho_{22}) - V_{01}\widetilde{\rho_{20}} - V_{20}\widetilde{\rho_{01}} e^{i\omega t} - i(\omega_2 - \omega_1 - \omega)\widetilde{\rho_{10}} \right\} \tag{101}$$

$$\tag{102}$$

IX. NONLINEAR SPECTROSCOPY IN A THREE-LEVEL SYSTEM

Based on the equations of the previous section we can now derive in a perturbative approach an expression for the third-order polarization in a three-level system. We will assume that the levels $|0\rangle$, $|1\rangle$, and $|2\rangle$ are similar to the lower three levels of a harmonic oscillator. Hence, we will take μ_{20} and thus V_{20} equal to zero. This also means that ρ_{22}

31

cannot be generated with less than four field interactions, meaning that terms involving ρ_{22} can also be neglected in the evaluation of the third-order polarization.

In a three-level system the third-order nonlinear polarization is not only given by $\rho_{10}^{(3)}$ but but also by $\rho_{21}^{(3)}$:

$$\rho_{21}^{(3)}(t) = -\frac{i\mu_{21}}{2\hbar} \int_{-\infty}^{t} dt_1 \left\{ E(t_1)\rho_{11}^{(2)}(t_1) - E^*(t_1)\rho_{20}^{(2)}(t_1) \right\} R(t - t_1) \tag{103}$$

Note that there are contributions from ρ_{22} and V_{20}. There are thus two contributions to $\rho_{21}^{(3)}$, coming from $\rho_{11}^{(2)}$ and $\rho_{20}^{(2)}$. This latter term can be created in a three-level system from:

$$\rho_{20}^{(2)}(t) = \frac{i\mu_{21}}{2\hbar} \int_{-\infty}^{t} dt_1 E(t_1)\rho_{10}^{(1)}(t_1) R_{20}(t - t_1), \tag{104}$$

where $R_{20}(t - t_1)$ includes the dephasing of the coherence of levels 0 and 2:

$$R_{20}(t - t_1) = e^{-i(2\omega - \omega_{01} - \omega_{12})(t - t_1)} e^{(t - t_1)/T_{2_{0 \to 2}}}. \tag{105}$$

This equation does not contain a term ρ_{21} because this density matrix element can only be generated by three field interactions and thus does not enter in a second-order contribution.

Finally, it should be noted that $\rho_{20}^{(2)}$ also contributes to $\rho_{10}^{(3)}$:

$$\rho_{10}^{(3)}(t) = -\int_{-\infty}^{t} dt_1 \left\{ \frac{i\mu_{10}}{2\hbar} E(t_1)(\rho_{00}^{(2)}(t_1) - \rho_{11}^{(2)}(t_1)) - \frac{i\mu_{21}}{2\hbar} E^*(t_1)\rho_{20}^{(2)} \right\} R(t - t_1) \tag{106}$$

These expressions imply that there are in total eight contributions to the third-order polarization, six contributing to $\rho_{10}^{(3)}$ and two to $\rho_{21}^{(3)}$. The eight contributions can be represented by Feynman diagrams as illustrated in Fig. 13.
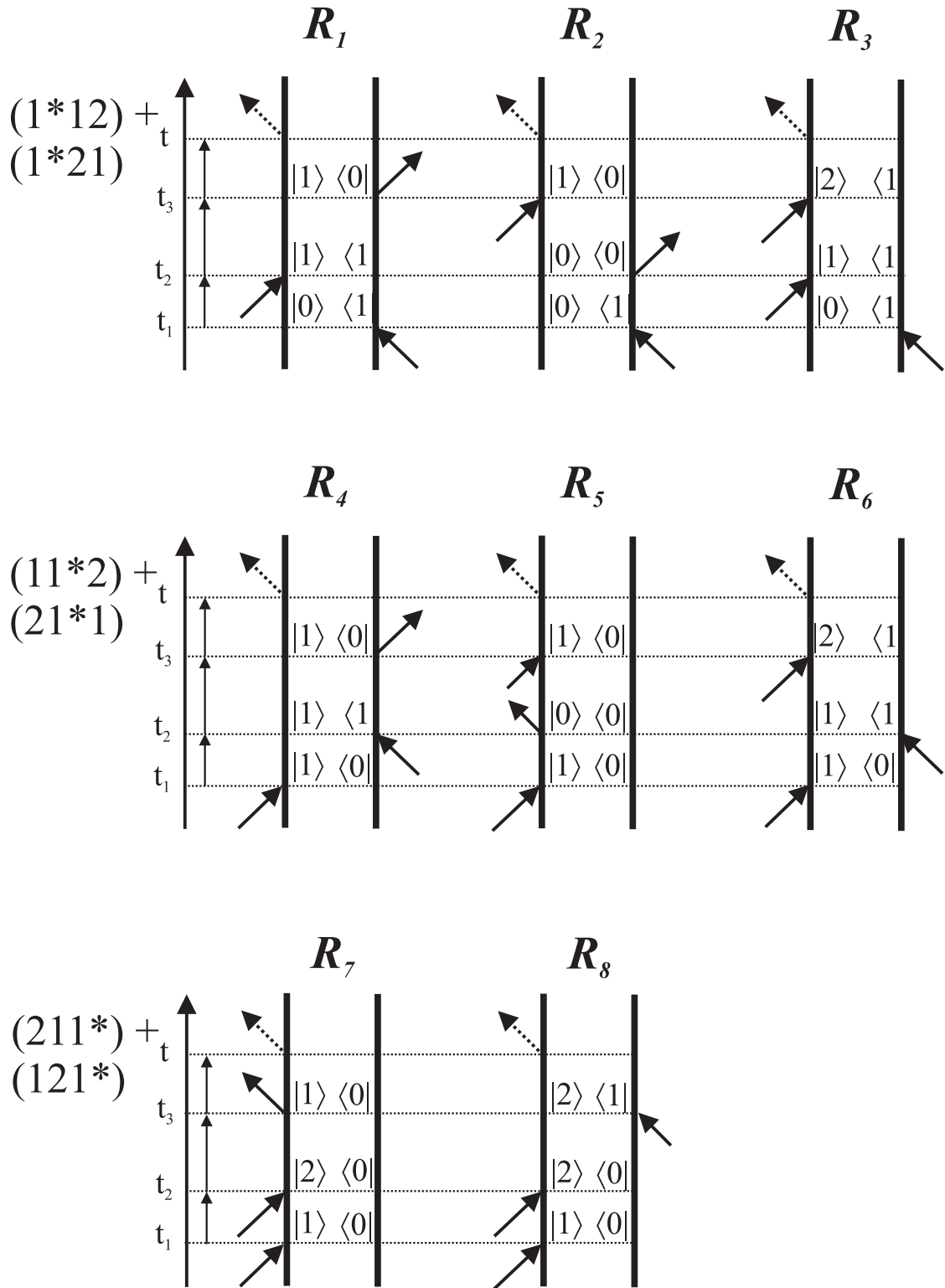
FIG. 13. Double-sided Feynman diagrams representing the field interactions and corresponding response functions for a three-level system. The symbols 1^*, 1, and 2 denote the fields E_1^*, E_1, and E_2, respectively, thereby representing the signal generated in pump-probe saturation spectroscopy.

A. Pump-probe saturation spectroscopy

In the case of a pump-probe experiment, two pulses are used: $\mathcal{E}_1(\mathbf{r}, t) = E_1 e^{i(\mathbf{k_1} \cdot \mathbf{r} - \omega_1 t)} +$ c.c. and $\mathcal{E}_2(\mathbf{r}, t) = E_2 e^{i(\mathbf{k_2} \cdot \mathbf{r} - \omega_1 t)} +$ c.c. with E_1 (the pump) being much stronger than E_2 (the probe). The generated $P^{(3)}$ in the direction of the probe ($\mathbf{k_2}$) is given by:

$$P^{(3)}(k_2, t) \propto \int_{-\infty}^{t} dt_3 \int_{-\infty}^{t_3} dt_2 \int_{-\infty}^{t_2} dt_1$$

$$(E_2(t_3)E_1(t_2)E_1^*(t_1) + E_1(t_3)E_2(t_2)E_1^*(t_1)) \times \sum_{1}^{3} R_i(t, t_3, t_2, t_1) +$$

$$(E_2(t_3)E_1^*(t_2)E_1(t_1) + E_1(t_3)E_1^*(t_2)E_2(t_1)) \times \sum_{4}^{6} R_i(t, t_3, t_2, t_1) +$$

$$(E_1^*(t_3)E_2(t_2)E_1(t_1) + E_1^*(t_3)E_1(t_2)E_2(t_1) \times \sum_{7}^{8} R_i(t, t_3, t_2, t_1) + \text{c.c.} \tag{107}$$

The R_i functions represent the response of the system, following a certain generation path (Feynman diagram) of generating the third-order polarization. In each of the eight paths there are two possible orders of the fields E_1 and E_2. Hence, the total number of field interactions giving rise to the third-order polarization in pump-probe saturation spectroscopy equals sixteen.

The ordinary (incoherent) pump-probe signal is represented by the (1*12) and (11*2) interactions (with 1, 1*, and 2 denoting the fields E_1, E_1^*, and E_2, respectively) and the response functions R_{1-6}. These interactions involve the excitation of the $v = 1$ state and a depletion of the $v = 0$ state by two subsequent interactions with the pump field. The excitation of $v = 1$ leads to $v = 1 \rightarrow 0$ stimulated emission. ($R_{1,4}$). The depletion of $v = 0$ leads to less $v = 0 \rightarrow 1$ absorption ($R_{2,5}$). Hence, both effects lead to an increased transmission at the $v = 0 \rightarrow 1$ transition frequency. In addition, the excitation of $v = 1$ by the pump leads to an induced absorption ($R_{3,6}$) at the ($v = 1 \rightarrow 2$) transition frequency (which can be observed at a frequency that is redshifted by approximately 300 cm^{-1} with respect to the $v = 0 \rightarrow 1$ absorption). The (1*21) and (21*1) interactions and the response functions R_{1-6} represent the excitation of a population grating (with wave vector $k_2 - k_1$) by the pump and probe fields. The diffraction of the pump field from this grating gives a signal

34

in the direction of the probe (k_2) that contributes to the coherent artefact. The generated $P^{(3)}(k_2, t)$ generates a field in the direction k_2 that interferes with the probe field E_2. The pump-induced change on the probe transmission is thus proportional to $E_2^* P^{(3)}(k_2, t)$+c.c.

The response functions R contain terms that reflect the population relaxation out of the levels $v = 1$ and $v = 2$ and the homogeneous dephasing of the coherence of the levels $v = 0$ and $v = 1$ and levels $v = 1$ and $v = 2$. The response functions have the following forms:

$$R_{1,2} = |\mu_{01}|^4 e^{-i(\omega-\omega_{01})(t-t_3-(t_2-t_1))} e^{-(t-t_3+(t_2-t_1))/T_{2_{0\to1}}} e^{-(t_3-t_2)/T_1} \tag{108}$$

$$R_3 = |\mu_{01}|^2 |\mu_{12}|^2 e^{-i(\omega-\omega_{01})(t_1-t_2)} e^{-i(\omega-\omega_{12})(t-t_3)}$$
$$e^{-(t_2-t_1)/T_{2_{0\to1}}} e^{-(t-t_3)/T_{2_{1\to2}}} e^{-(t_3-t_2)/T_1}$$

$$R_{4,5} = |\mu 01|^4 e^{-i(\omega-\omega_{01})(t-t_3+(t_2-t_1))} e^{-(t-t_3+(t_2-t_1))/T_{2_{0\to1}}} e^{-(t_3-t_2)/T_1}$$

$$R_6 = |\mu_{01}|^2 |\mu_{12}|^2 e^{-i(\omega-\omega_{01})(t_2-t_1)} e^{-i(\omega-\omega_{12})(t-t_3)}$$
$$e^{-(t_2-t_1)/T_{2_{0\to1}}} e^{-(t-t_3)/T_{2_{1\to2}}} e^{-(t_3-t_2)/T_1}$$

$$R_7 = |\mu_{01}|^2 |\mu_{12}|^2 e^{-i(\omega-\omega_{01})(t-t_3+(t_2-t_1))} e^{-i(2\omega-\omega_{01}-\omega_{12})(t_3-t_2)}$$
$$e^{-(t-t_3+(t_2-t_1))/T_{2_{0\to1}}} e^{-(t_3-t_2)/T_{2_{0\to2}}}$$

$$R_8 = |\mu_{01}|^2 |\mu_{12}|^2 e^{-i(\omega-\omega_{01})(t_2-t_1)} e^{-i(2\omega-\omega_{01}-\omega_{12})(t_3-t_2)} e^{-i(\omega-\omega_{12})(t-t_3)}$$
$$e^{-(t_2-t_1)/T_{2_{0\to1}}} e^{-(t-t_3)/T_{2_{1\to2}}} e^{-(t_3-t_2)/T_{2_{0\to2}}}$$

with μ_{ij} the transition dipole moment of the $v = i \to j$ transition, ω_{ij}, the resonance frequency of this transition, and $T_{2_{i\to j}}$ the dephasing time of this transition. The functions R_{1-6} also contain a term representing the population relaxation out of level $v = 1$.
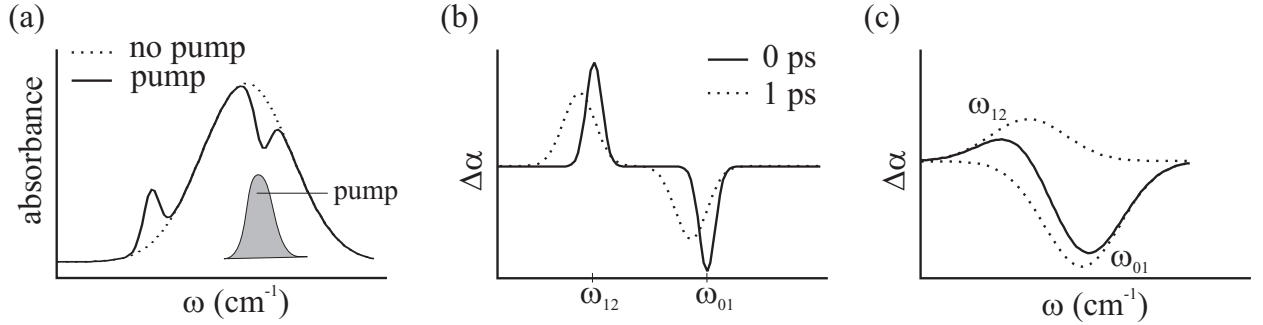
X. INHOMOGENEOUS BROADENING AND SPECTRAL DIFFUSION

FIG. 14. Inhomogeneous broadening and spectral diffusion. a) A pump pulse that is narrower than the width of an inhomgeneously broadened absorption band will burn a hole in it. b) At zero delay the transient spectrum will show bleaching and induced absorption features, the widths of which are determined by the pump pulse. As the pump-probe delay is increased frequency fluctuations will lead to the broadening and shifting of the transient spectrum until it reaches its equilibrium shape. c) Typical shape of the transient spectrum of water. The bleaching and induced absorption (dotted lines) are broadened to such extent that they overlap. The solid line represents the sum of the bleaching and induced absorption.

In the foregoing discussions it was implicitly assumed that infrared absorption lines are homogeneously broadened. This means that every molecule has essentially the same absorption spectrum. The bandwidth over which a single molecule absorbs radiation is referred to as the homogeneous linewidth of the particular transition. However, infrared absorption bands can also be inhomogeneously broadened, an example of which is the OH stretching vibration in liquid water. In this case the broadening of the absorption arises because different molecules absorb at different center frequencies. In linear spectroscopy homogeneous and inhomogeneous broadening cannot be distinguished; in pump-probe spectroscopy, on the other hand, the difference is immediately clear.

Figure 14 exemplifies this issue. We investigate the effect of using a pump-pulse that has a narrower frequency distribution than the (inhomogeneously broadened) absorption band. Since the absorption band consists of species that absorb at different center frequencies,

rather than of a single species that absorbs over a wide frequency interval, not all molecules are resonant with the pump pulse. As a result only part of the absorption band is bleached (figure 14a) and the spectrum after excitation by the pump will have a hole in it. As a consequence of this effect the transient spectrum can be narrower than the linear spectrum. In this case pump-probe spectroscopy is sometimes also referred to as hole-burning spectroscopy.

The variation in the center frequencies is due to the different environments of the various molecules. In a liquid these environments interconvert on a characteristic timescale and this causes the absorption frequency of a particular molecule to fluctuate in time. If a narrow-band pulse is used to excite the sample, this will lead to the excitation of a non-equilibrium distribution of transition frequencies. The transient spectrum will therefore broaden upon increasing the pump-probe delay until it reaches the equilibrium shape. The rate at which the transient spectrum broadens provides a way to determine the timescale of the frequency fluctuations.

Finally we point out that in the case of inhomogeneous broadening the width of absorption bands can be so large that ground state bleach and induced absorption overlap. This is the case for the OH stretch vibration of water. Figure 14c displays the characteristic lineshape that this leads to.

A. Photon-echo spectroscopy

In a three-pulse photon-echo experiment, the interacting fields E_1, E_2 and E_3 have a comparable amplitude. In this case, pulses with wave vectors k_1, k_2 and k_3 are combined to generate a third-order polarization $P^{(3)}$ in the direction $k_3 + k_2 - k_1$. This $P^{(3)}$ is given by:

$$P^{(3)}(k_3 + k_2 - k_1, t) \propto \int_{-\infty}^{t} dt_3 \int_{-\infty}^{t_3} dt_2 \int_{-\infty}^{t_2} dt_1$$

$$(E_3(t_3)E_2(t_2)E_1^*(t_1) + E_2(t_3)E_3(t_2)E_1^*(t_1)) \times \sum_{1}^{3} R_i(t, t_3, t_2, t_1) +$$

$$(E_3(t_3)E_1^*(t_2)E_2(t_1) + E_2(t_3)E_1^*(t_2)E_3(t_1)) \times \sum_{4}^{6} R_i(t, t_3, t_2, t_1) +$$

$$(E_1^*(t_3)E_3(t_2)E_2(t_1) + E_1^*(t_3)E_2(t_2)E_3(t_1)) \times \sum_{7}^{8} R_i(t, t_3, t_2, t_1) + \text{c.c.} \qquad (109)$$

In a photon-echo experiment, the field generated by $P^{(3)}(k_3 + k_2 - k_1, t)$ can be detected background-free. In a photon-echo experiment there exists an inhomogeneous distribution of oscillators that for some configurations and orders of interactions can show a rephasing effect. The overall third-order polarization is a sum of the third-order polarizations of the individual oscillators. In the response functions we have to replace the resonance frequencies ω_{01} and ω_{12} by distributions of resonance frequencies: $\int d\omega_{01,i} G(\omega_{01,i})$ and $\int d\omega_{12,i} G(\omega_{12,i})$. If we assume that these distributions are correlated, meaning that $\omega_{12,i} - \omega_{12} = \omega_{01,i} - \omega_{01} = \delta\omega_i$, we obtain the following response functions:

$$R_{1,2} = \int \delta\omega_i G(\delta\omega_i) |\mu_{01}|^4 e^{-i(\omega - \omega_{01} - \delta\omega_i)(t - t_3 - (t_2 - t_1))} e^{-(t - t_3 + (t_2 - t_1))/T_{2_{0\to1}}} e^{-(t_3 - t_2)/T_1} \qquad (110)$$

$$R_3 = \int \delta\omega_i G(\delta\omega_i) |\mu_{01}|^2 |\mu_{12}|^2 e^{-i(\omega - \omega_{01} - \delta\omega_i)(t_1 - t_2)} e^{-i(\omega - \omega_{12} - \delta\omega_i)(t - t_3)}$$
$$e^{-(t_2 - t_1)/T_{2_{0\to1}}} e^{-(t - t_3)/T_{2_{1\to2}}} e^{-(t_3 - t_2)/T_1}$$

$$R_{4,5} = \int \delta\omega_i G(\delta\omega_i) |\mu 01|^4 e^{-i(\omega - \omega_{01} - \delta\omega_i)(t - t_3 + (t_2 - t_1))} e^{-(t - t_3 + (t_2 - t_1))/T_{2_{0\to1}}} e^{-(t_3 - t_2)/T_1}$$

$$R_6 = \int \delta\omega_i G(\delta\omega_i) |\mu_{01}|^2 |\mu_{12}|^2 e^{-i(\omega - \omega_{01} - \delta\omega_i)(t_2 - t_1)} e^{-i(\omega - \omega_{12} - \delta\omega_i)(t - t_3)}$$
$$e^{-(t_2 - t_1)/T_{2_{0\to1}}} e^{-(t - t_3)/T_{2_{1\to2}}} e^{-(t_3 - t_2)/T_1}$$

$$R_7 = \int \delta\omega_i G(\delta\omega_i) |\mu_{01}|^2 |\mu_{12}|^2 e^{-i(\omega - \omega_{01} - \delta\omega_i)(t - t_3 + (t_2 - t_1))} e^{-i(2\omega - \omega_{01} - \omega_{12} - 2\delta\omega_i)(t_3 - t_2)}$$
$$e^{-(t - t_3 + (t_2 - t_1))/T_{2_{0\to1}}} e^{-(t_3 - t_2)/T_{2_{0\to2}}}$$

$$R_8 = \int \delta\omega_i G(\delta\omega_i) |\mu_{01}|^2 |\mu_{12}|^2 e^{-i(\omega - \omega_{01} - \delta\omega_i)(t_2 - t_1)} e^{-i(2\omega - \omega_{01} - \omega_{12} - 2\delta\omega_i)(t_3 - t_2)} e^{-i(\omega - \omega_{12} - \delta\omega_i)(t - t_3)}$$
$$e^{-(t_2 - t_1)/T_{2_{0\to1}}} e^{-(t - t_3)/T_{2_{1\to2}}} e^{-(t_3 - t_2)/T_{2_{0\to2}}}$$

The field interactions and the response functions for a photon-echo experiment are depicted schematically in Fig. 15.

$$R_1 \qquad R_2 \qquad R_3$$

(1*23) +t
(1*32)

t_3

t_2

t_1

R_1	R_2	R_3
$\lvert 1\rangle \langle 0\rvert$	$\lvert 1\rangle \langle 0\rvert$	$\lvert 2\rangle \langle 1$
$\lvert 1\rangle \langle 1$	$\lvert 0\rangle \langle 0\rvert$	$\lvert 1\rangle \langle 1$
$\lvert 0\rangle \langle 1$	$\lvert 0\rangle \langle 1$	$\lvert 0\rangle \langle 1$

$$R_4 \qquad R_5 \qquad R_6$$

(21*3) +t
(31*2)

t_3

t_2

t_1

R_4	R_5	R_6
$\lvert 1\rangle \langle 0\rvert$	$\lvert 1\rangle \langle 0\rvert$	$\lvert 2\rangle \langle 1$
$\lvert 1\rangle \langle 1$	$\lvert 0\rangle \langle 0\rvert$	$\lvert 1\rangle \langle 1$
$\lvert 1\rangle \langle 0\rvert$	$\lvert 1\rangle \langle 0\rvert$	$\lvert 1\rangle \langle 0\rvert$

$$R_7 \qquad R_8$$

(231*) +t
(321*)

t_3

t_2

t_1

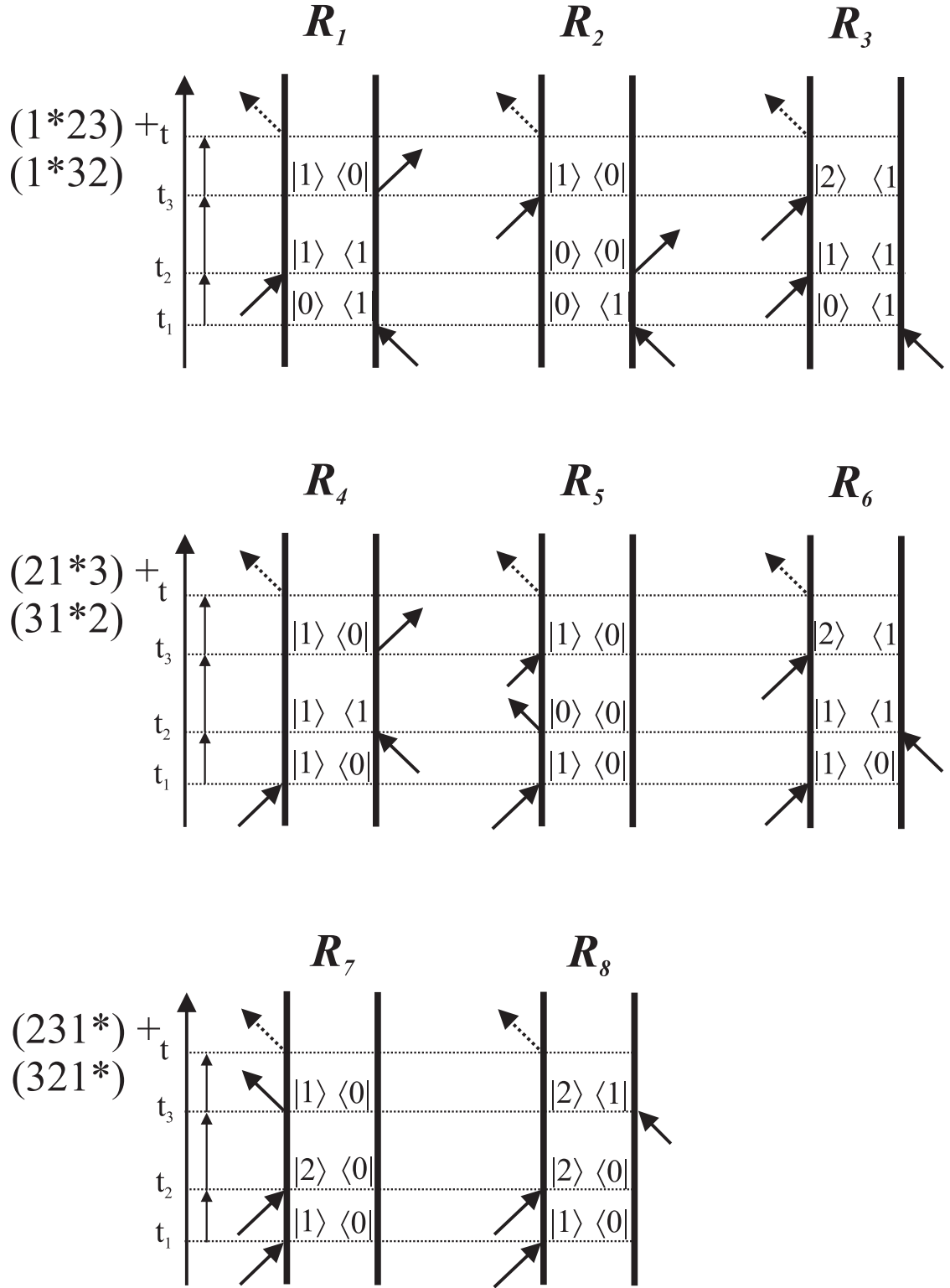| R_7	R_8
$\lvert 1\rangle \langle 0\rvert$	$\lvert 2\rangle \langle 1\rvert$
$\lvert 2\rangle \langle 0\rvert$	$\lvert 2\rangle \langle 0\rvert$
$\lvert 1\rangle \langle 0\rvert$	$\lvert 1\rangle \langle 0\rvert$

FIG. 15. Double-sided Feynman diagrams representing the field interactions and corresponding response functions in three-pulse photon-echo spectroscopy, giving a signal in the direction $k_3 + k_2 - k_1$. The symbols 1*, 2, and 3 denote the fields E_1^*, E_2, and E_3, respectively.

The photon-echo signal can also be generated by two pulses. In this case field E_2 performs two of the three field interactions giving rise to a signal in the direction $2k_2 - k_1$. In the limit of very short pulses, only the first terms with response functions R_{1-3} are important. Variation of the signal as a function of the time between the pulses gives information on the homogeneous dephasing time constants $T_{2_{0 \to 1}}$ and $T_{2_{1 \to 2}}$.

The functions R_i differ in their rephasing characteristics. For inhomogeneously broadened transitions, R_{1-3} describe a rephasing effect, R_{4-8} do not. This becomes clear if we consider the frequency dependent terms in the response function. The response functions $R_{1,2}$ contain the term $e^{-i(\omega - \omega_{01} - \delta\omega_i)(t - t_3 - (t_2 - t_1))}$. It follows that for $(t - t_3) = (t_2 - t_1)$, the third-order polarizations are in phase generating the so-called photon-echo signal. The origin of this effect is that the first field interaction was with E_1^* contributing a wave vector $-k_1$ to the population grating with wave vector $k_2 - k_1$ and the third-order polarization with wave vector $k_3 + k_2 - k_1$. This means that the phase evolution of the first-order polarization generated by E_1^* in the time interval between t_1 and t_2 is the complex conjugate of the phase evolution of the third-order polarization between t_3 and t. Hence, the accumulated relative phase $-\delta\omega_i(t_2 - t_1)$ of the oscillator with resonance frequency $\omega_{01} + \delta\omega_i$ can be compensated by $\delta\omega_i(t - t_3)$ in the third-order polarization. As this is the case for all oscillators within the inhomogeneous distribution $G(\delta\omega_i)$, all oscillators become in phase at t, leading to a macroscopic third-order polarization that acts as source term in the wave equation to emit a light pulse. This light pulse is denoted a photon echo as it is emitted at a time after the third pulse that is equal to the time difference between the first two pulses.

An interesting issue is how the phase information is stored during the time period of the population grating. The relative phase between the second field and the polarization generated by the first field interaction determines whether population is further pumped up to the excited state or rather being pumped back to the ground state. As the wave vectors of the first and the second field interactions have different direction, this phase difference depends on the transverse position on the sample. As a result, a population grating is formed. The phase difference also depends on the phase accumulation of the polarization

generated by the first field interaction, i.e. on the resonance frequency of the oscillator. This means that for $t_2 - t_1 > 0$ the population gratings associated with the different oscillators will differ in transverse phase. Between the second and the third field interaction there is no further phase accumulation and the differences in accumulated phase are stored in the form of the transverse phase shifts of the population gratings.

The generation of the photon echo requires that the oscillator remains at the same frequency position within the inhomogeneous distribution at all times. Often however, there are spectral diffusion processes. In this case the photon-echo signal can be used to measure the time scale of the spectral diffusion. In case the inhomogeneous distribution is static, the photon-echo signal is practically independent of the time interval $t_3 - t_2$, except for the often relatively slow population relaxation. However, if there is spectral diffusion, the photon-echo signal will be dependent on the length of the time interval $t_3 - t_2$, because a change of the resonance frequency during this time will make the rephasing impossible thus leading to a decrease of the photon echo signal. The photon-echo signal as a function of $t_3 - t_2$ can thus give information on the spectral diffusion, provided that the contribution to the decay of the signal due to population relaxation is known.

In the liquid phase there is often not a clear distinction between homogeneous and inhomogeneous line-broadening contributions. Here the dynamics is often influenced by spectral diffusion with a time constant that is comparable to the pulse duration and/or the lifetime T_1 of the excitation. In this case, the response functions R_i become more complicated and should be evaluated using a more advanced description, like for instance the Gauss-Markov model or the Brownian oscillator model.

XI. POLARIZATION-RESOLVED NONLINEAR SPECTROSCOPY

Until now it was silently assumed that the excited molecules are distributed isotropically. However, in reality the distribution of excited molecules is anisotropic because molecules that have their transition dipole moments aligned parallel to the pump polarization are

excited preferentially (figure 16a). As a consequence the amplitude of the pump-probe response depends on the relative polarizations of the pump and probe pulses (figure 16b). For parallel pump and probe polarizations the response is initially larger than for perpendicular polarizations (because the concentration of excited molecules is zero for molecules that have their transition dipole moments perpendicular to the pump polarization). The orientational motion of the excited molecules scrambles their orientations and eventually causes their distribution to become isotropic. As a consequence the parallel signal decays faster than the perpendicular signal and this continues until the two signals are identical. At this point the excited molecules have lost all memory of their initial orientations. It is clear that the rate at which the difference between the parallel and perpendicular signals decays is determined by the orientational motion of the molecules .
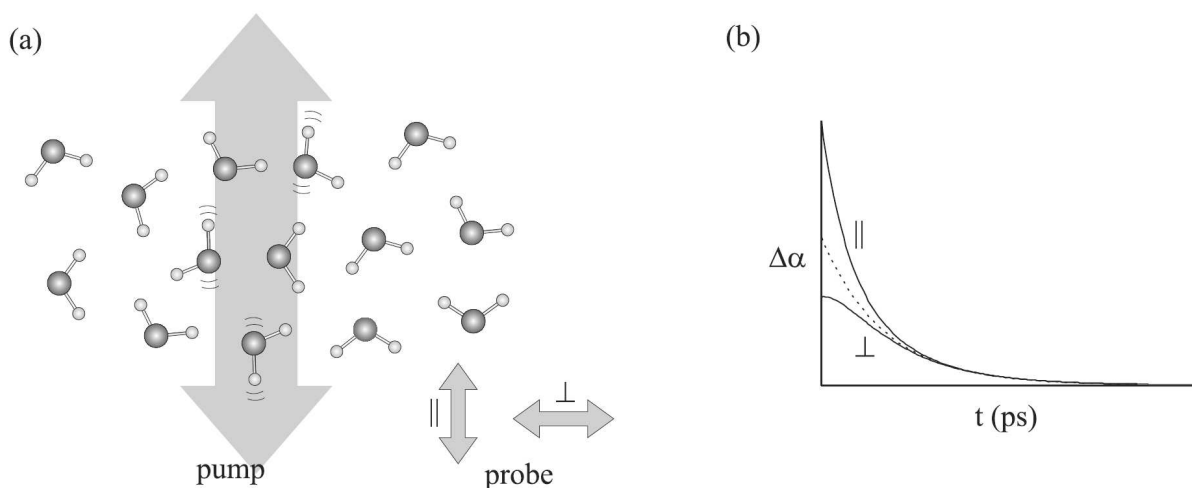

FIG. 16. a) Preferential excitation of molecules that have their transition dipole moments parallel to the pump pulse polarization. b) Delay scan of the parallel and perpendicular signals. The dotted line shows the signal if the orientations of the excited molecules were distributed isotropically. The parallel signal is initially higher than the isotropic signal but decays faster; the perpendicular signal is initially lower than the isotropic signal but decays more slowly.
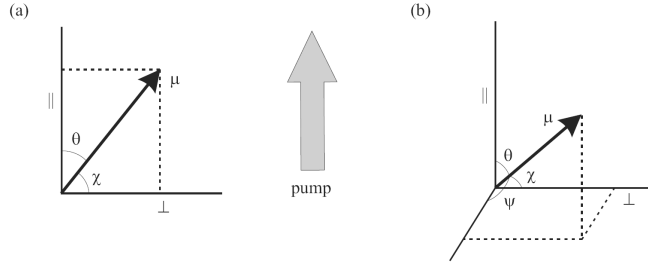
A. Isotropic signal

FIG. 17. Contribution of a single dipole to the parallel and perpendicular pump-probe signals in two dimensions (a) and in three dimensions (b).

Both the parallel and perpendicular response shown in figure 16b are affected by the orientational motion of the molecules, which is inconvenient if one wants to study vibrational relaxation. It would be more convenient to dispose of a response such as the dotted line in figure 16 which depends only on the total concentration of excited molecules. This response is referred to as the isotropic response. It may seem that averaging the parallel and perpendicular responses would yield the isotropic response. However, it turns out that this is only correct if molecules rotate in two dimensions. In three dimensions the isotropic response is found by weighing the perpendicular response more heavily,

$$\Delta\alpha_{\mathrm{iso}} = \frac{\Delta\alpha_{||} + 2\Delta\alpha_\perp}{3}, \tag{111}$$

where $\Delta\alpha_{||}$ and $\Delta\alpha_\perp$ are the absorption changes when the pump and probe beams are polarized parallel and perpendicular to each other, respectively. This equation can be rationalized with the help of figure 17. We first consider the two dimensional situation. A single excited dipole $\vec{\mu}$ contributes to the induced absorptions of both the parallel and perpendicular responses according to

$$\Delta\alpha_{||} \propto \cos^2\theta, \tag{112}$$

$$\Delta\alpha_\perp \propto \cos^2\chi. \tag{113}$$

43

It is directly clear that the sum of these two signals does not depend on the orientation of the dipole. Therefore in two dimensions the isotropic signal is given by the simple average of the parallel and perpendicular signals.

In three dimensions the quantity that is independent of orientation is $\cos^2 \theta + \cos^2 \chi + \cos^2 \psi$ (figure 17b) so that the absorption needs to be probed in three orthogonal directions to obtain the isotropic response. Experimentally this would not be very straightforward but fortunately matters are simplified by the cylindrical symmetry of the sample after excitation. As a result of this symmetry the *average* responses are equal for the two perpendicular probe directions, so that $\langle \cos^2 \theta + 2 \cos^2 \chi \rangle$ is the quantity that is independent of orientation. This explains the form of eqn. 111.

In order to prepare for the coming discussion we also show how the above conclusion can be reached by considering the distribution of excited molecules $N(\theta, \phi, t)$. Immediately after excitation this distribution is given by

$$N(\theta, \phi, t) = g(\theta, \phi, t)N_1, \tag{114}$$

where N_1 represents the total concentration of excited molecules as it did in the previous sections and $g(\theta, \phi, t)$ is the function that represents the orientational distribution of excited molecules. $g(\theta, \phi, t)$ has a number of properties:

- Being a distribution function it is normalized at all times

$$\int g(\theta, \phi, t) \, d\Omega = 1, \tag{115}$$

  where the integral runs over the unit sphere and $d\Omega = \sin \theta \, d\theta \, d\phi$ is the surface element in spherical coordinates.

- At zero delay its functional forms is determined by the excitation probability

$$g(\theta, \phi, 0) = \frac{3}{4\pi} \cos^2 \theta. \tag{116}$$

- In the limit of long delay times it evolves to an isotropic distribution

$$\lim_{t \to \infty} g(\theta, \phi, t) = \frac{1}{4\pi}. \tag{117}$$

- Finally, in an isotropic sample $g(\theta, \phi, t)$ is a function of only the polar angle

$$g(\theta, \phi, t) = \frac{g_\theta(\theta, t)}{2\pi}, \tag{118}$$

where $g_\theta(\theta, t)$ is the distribution function of the polar coordinate. The factor 2π enters to ensure its normalization

$$\int_0^\pi g_\theta(\theta, t) \sin \theta \, d\theta = 1. \tag{119}$$

The parallel and perpendicular absorption changes can be expressed in terms of integrals over the distribution function

$$\Delta \alpha_{||}(t) = 3\sigma_{12} N_1 \int g(\theta, \phi, t) \cos^2 \theta \, d\Omega, \tag{120}$$

$$\Delta \alpha_\perp(t) = 3\sigma_{12} N_1 \int g(\theta, \phi, t) \sin^2 \theta \sin^2 \phi \, d\Omega, \tag{121}$$

where in the second equation we have used the fact that $\cos^2 \chi = \sin^2 \phi \sin^2 \theta$. The factor of 3 enters because the cross section is defined as the average (i.e. isotropic) cross section, which is three times as small as its maximum value. The independence of the isotropic signal on the distribution function can be shown as follows

$$\Delta \alpha_{\text{iso}}(t) = \frac{1}{3}(\Delta \alpha_{||}(t) + 2\Delta \alpha_\perp(t)), \tag{122}$$

$$= \sigma_{12} N_1 \int g(\theta, \phi, t)(\cos^2 \theta + 2\sin^2 \theta \sin^2 \phi) \, d\Omega. \tag{123}$$

We use the fact that the sample is isotropic and integrate over the azimuthal coordinate,

$$\Delta \alpha_{\text{iso}}(t) = \sigma_{12} N_1 \int \frac{g_\theta(\theta, t)}{2\pi}(\cos^2 \theta + 2\sin^2 \theta \sin^2 \phi) \, d\Omega, \tag{124}$$

$$= \sigma_{12} N_1 \int_0^\pi g_\theta(\theta, t) \sin \theta \, d\theta, \tag{125}$$

$$= \sigma_{12} N_1. \tag{126}$$

45

This definition of the isotropic signal ensures that all the equations introduced in the previous paragraphs remain valid if $\Delta\alpha$ denotes the isotropic signal. The isotropic signal reflects the dynamics due to vibrational relaxation and spectral diffusion but is independent of any orientational processes.

B. Anisotropy

It has been demonstrated that the difference between the parallel and perpendicular absorption changes contains information about the orientational dynamics of molecules. A quantity that depends *exclusively* on the orientational dynamics is obtained by normalizing this difference to the total signal

$$R(t) = \frac{\Delta\alpha_{||} - \Delta\alpha_{\perp}}{\Delta\alpha_{||} + 2\Delta\alpha_{\perp}}. \tag{127}$$

This is the anisotropy, which we shall employ frequently throughout this thesis to study the orientational motion of water molecules.

In terms of the orientational distribution function $g(\theta, \phi, t)$ the anisotropy reads

$$R(t) = \int g(\theta, \phi, t)(\cos^2\theta - \sin^2\theta\sin^2\phi)\,d\Omega. \tag{128}$$

This expression shows that the anisotropy does indeed only reflect the orientational motion of molecules, as required. However, as it stands the expression is not very convenient.
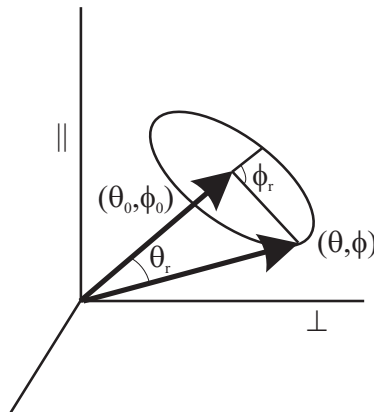

FIG. 18. Polar coordinates used to define the initial and final orientations of a dipole. The coordinates (θ_r, ϕ_r) are defined relative to the initial coordinates (θ_0, ϕ_0).

In the following we will rewrite the expression for the anisotropy in such a way that it reflects the motion of individual molecules.

The orientational diffusion of the ensemble of aqueous solvation shells that are excited by the pump pulse is described by the equation

$$\frac{\partial n(\theta,t)}{\partial t} = \frac{D_\theta}{\sin\theta} \frac{\partial}{\partial\theta} \left(\sin\theta \frac{\partial n(\theta,t)}{\partial\theta} \right), \tag{129}$$

with θ the angle with respect to the pump-pulse polarization, $n(\theta,t)d\Omega$ the number of particles in a solid angle $d\Omega$ ($d\Omega = d\phi d\theta \sin\theta$), ϕ the azimuth angle, and D_θ the orientational diffusion constant. Equation (1) does not contain any dependence on the azimuth angle ϕ, because the excitation is symmetric around the pump-pulse polarization axis. The solution of this equation can be written as a sum of exponentially decaying Legendre polynomials P_l:

$$n(\theta,t) = \sum_{l\geq 0} a_l P_l(\cos\theta) e^{-D_\theta l(l+1)t}, \tag{130}$$

with a_l the coefficients that are determined by the distribution of $n(\theta,t)$ at t=0. The initial distribution is given by:

$$g(\theta,\phi,0) = \frac{3}{4\pi} \cos^2\theta \tag{131}$$

The solution of the orientational diffusion equation is thus given by

$$g(\theta,\phi,t) = \frac{1}{4\pi} \left[3\cos^2\theta - 1)e^{-t/6D} + 1 \right] \tag{132}$$

The rotational anisotropy is the difference between $\cos^2\theta$ and $\sin^2\theta\cos^2\phi$ weighted with the distribution function $g(\theta,\phi,t)$.:

$$R(t) = \frac{\int\int d\Omega(\cos^2\theta - \sin^2\theta\cos^2\phi)g(\theta,\phi,t)}{\int\int d\Omega(\cos^2\theta + 2\sin^2\theta\cos^2\phi)g(\theta,\phi,t)} = \frac{2}{5}e^{-t/6D} = \frac{2}{5}e^{-t/\tau_{or}} \tag{133}$$

The measured anisotropy $R(\tau)$ thus equals $\langle P_2(\cos\theta)\rangle$, and the time constant τ_{or} of the decay of $R(\tau)$ is related to D_θ by $\tau_{\mathrm{or}} = 1/(6D_\theta)$. The orientational diffusion constant D_θ can be related to the viscosity of the liquid using the Stokes-Einstein relation for orientational diffusion of a sphere:

$$D_\theta = \frac{kT}{8\pi\eta(T)r_{hyd}^3}, \qquad (134)$$

with k Boltzmann's constant, T the temperature in Kelvin, $\eta(T)$ the temperature-dependent viscosity, and r_{hyd} the hydrodynamic radius of the reorienting molecules. Combining this equation with $\tau_{or} = 1/(6D_\theta)$ gives:

$$\tau_{or}(T) = \frac{4\pi\eta(T)r_{hyd}^3}{3kT}. \qquad (135)$$